A yeast two-hybrid screen identifies a novel interactor of the TRAPP subunit sedlin

Sokunthear Hul

A Thesis in the department of Biology

Presented in Partial Fulfillment of the Requirements

For the Degree of Master of Science (Biology) at

Concordia University

Montreal, Quebec, Canada

January 2010

Your file Votre référence
ISBN: 978-0-494-67246-4
Our file Notre référence
ISBN: 978-0-494-67246-4

Abstract

A yeast two-hybrid screen identifies a novel interactor of the TRAPP subunit sedlin

Sokunthear Hul

Sedlin is implicated in a diverse set of cellular roles that include membrane trafficking and gene regulation. Mutations in sedlin lead to a skeletal disorder called SEDT. However, a complete understanding of the function(s) of sedlin remains elusive. Sedlin is one component of a large heteromeric complex called TRAPP (transport protein particle) that is involved in membrane traffic between the endoplasmic reticulum and the Golgi. To begin to characterize the function of sedlin a yeast two-hybrid (Y2H) screen was performed. This screen identified a novel sedlin interactor called SPATA4. The interaction was confirmed both *in vitro*, using an MBP-pulldown assay, and *in vivo*, using coimmunoprecipitation. A gel filtration experiment showed that SPATA4 co-fractionates with the TRAPP complex, a result that was supported by *in vitro* work. Since SPATA4 was originally identified as a protein involved in spermatogenesis, the interaction between TRAPP and SPATA4 may suggest a specialized role for TRAPP and/or TRAPP isocomplexes in spermatogenesis. Alternatively, SPATA4 may play a previously unreported role in membrane traffic. A bioinformatic analysis of SPATA4 revealed a domain found in another potential sedlin-interactor called SPEF1. A portion of this domain is known to mediate interaction with microtubules. Taken together, the SPATA4-TRAPP interaction may link the TRAPP vesicle tethering complex to the cytoskeleton which transports Golgi-destined vesicles.

Acknowledgements

There are many people to whom I owe a debt of gratitude for their patience, wisdom, guidance, help and support throughout this amazing and unforgettable journey. First and foremost, thank you Dr. Michael Sacher. You are the best supervisor ever. To my committee members, Dr. P. Joyce and Dr. W. Zerges, thank you for your time, help and guidance. To Dr. A. Piekny, thank you for the plasmid construct, your troubleshooting advice and for taking the time to help me. To all the members of the Sacher Lab (including the honorary members), there is too much to thank you guys for so I'll just say thank you for everything. In particular, I'd like to thank Dr. James Scrivens for all of his help, encouragement and guidance. And last but not least, I'd like to thank my family and friends for all of their unconditional love and support. Without you guys I would not be where or who I am today!

Table of Contents

List of Figures

List of Tables

List of Abbreviations

3AT: 3-amino-1,2,4-triazole

aa: amino acid

AD: activation domain

ARC: arthrogryposis-renal dysfunction-cholestasis

BD: binding domain

BLAST: Basic Local Alignment Search Tool

CDS: coding sequence

CH: calponin homology

CLIC: chloride intracellular channel protein

COG: conserved oligomeric Golgi

CoIP: coimmunoprecipitation

CORVET: class C core vacuole/endosome tethering

DDO: double drop out

DMEM: Dulbecco's modified Eagle Medium

DUF1042: domain of unknown function

ECL: enhanced chemiluminescent

E. coli: Escherichia coli

ECT2: epithelial cell transforming sequence 2

EH: epsin homology

EM: electron microscope

ER: endoplasmic reticulum

FBS: fetal bovine serum

GAP: GTPase activating protein

GARP: Golgi-associated retrograde protein

GDP: guanosine diphosphate

GEF: guanine nucleotide exchange factor

GTP: guanosine triphosphate

HD: Huntington's disease

HEK 293T: human embryonic kidney 293T cells

HBS: Hepes buffered saline

HOPS: homotypic fusion and vacuole protein sorting

LHβ: luteinizing hormone β

LB: luria broth

MBP-1: c-myc promoter-binding protein 1

ORF: open reading frame

PBS: phosphate buffer saline

PBSt: phosbate buffer saline containing 0.2% Tween

PCR: polymerase chain reaction

PM: plasma membrane

P/S: penicillin/streptomycin

PVDF: polyvinylidenefluoride

QDO: quadruple drop out

RRS: RAS-recruitment systems

RT: room temperature

SB: sample buffer

SDS-PAGE: sodium dodecyl sulphate – polyacrylamide gel electrophoresis

SEDT: Spondyloepiphyseal dysplasia tarda

SNAP-25: soluble N-ethylmaleimide-sensitive factor attachment protein receptor (SNARE) protein

SNARE: soluble N-ethylmaleimide-sensitive factor attachment protein receptor

SPATA4: spermatogenesis associated 4

SPEF: sperm flagellar protein

SPR: surface plasmon resonance

SRG2: spermatogenesis related gene

SRS: SOS-recruitment systems

TDO: triple drop out

TRAPP: Transport Protein Particle

TRAPPC2L: TRAPPC2-like

TSARG2: testis and spermatogenesis protein 2

t-SNARE: target SNARE

v-SNARE: vesicle-SNARE

Y2H: yeast two-hybrid screen

1. Introduction

1.1 Membrane Trafficking

In every eukaryotic cell a highly regulated and precise system controls the flow of proteins and lipids to the correct membrane-bound compartment. This important process is termed membrane trafficking and is essential in maintaining the identity of all organelles. Within a cell the main mode of trafficking is vesicular transport. In the latter case cargo is loaded into a vesicle and the vesicle travels to its destination where it will then fuse with the acceptor membrane and deliver its cargo. Since there are many membrane-bound compartments within a cell, consequently there are many potential places for a vesicle to incorrectly deliver its cargo. In order to avoid this, vesicular transport is a highly regulated process and consists of many factors that each contribute to ensure that each vesicle reaches the correct destination. These factors include Rabs, guanine nucleotide exchange factor (GEFs), tethers, and soluble N-ethylmaleimide-sensitive factor attachment protein receptors (SNAREs) whose identities vary depending on the trafficking pathway (Pfeffer, 1999). In the pathway between the endoplasmic reticulum (ER) and the Golgi, the formation of the vesicle begins with the recruitment of the COP II coat components onto the ER membrane; the transmembrane-anchored and ER-resident protein, Sec12 recruits the GTPase, Sar1 onto the ER membrane. Binding of Sar1 to the ER then allows the GTPase activating protein (GAP), Sec23 and the cargo recruiter, Sec24 to form a complex with Sar1. Finally, deformation of the membrane and

stabilization of the polymerizing coat occurs after binding of the Sec13/31 complex to the Sec23/24 complex (Matsuoka et al., 1998; Bielli et al., 2005). Once formed, the vesicle then travels to the Golgi where extended coiled-coil proteins such as p115, GM130/golgin-95 in mammalian cells and Uso1p in yeast interact with the coat proteins and tether the vesicle to the target membrane. Further specificity is established by a second tethering action carried out by the multi-subunit tethering complex called *Tra*nsport *P*rotein *P*article (TRAPP) (Kim et al., 2006). Fusion of the vesicle and target membrane then occurs subsequent to SNARE interactions that form a highly stable SNAREpin complex, composed of one SNARE from the vesicle and three SNAREs from the target membrane. The SNAREs found on the vesicle and the target membrane are called v- and t-SNAREs respectively (vesicle- and target SNAREs) or they may also be referred to as R- and Q-SNAREs respectively, where the latter terminology refers to a conserved residue essential to the formation of a stable SNAREpin complex (Fasshauer et al., 1998). At this point, vesicular trafficking is complete since the vesicle has successfully reached its target membrane and fused at the appropriate destination.

1.2 Membrane Trafficking and Diseases

The eukaryotic cell contains several membrane-bound compartments that each perform a unique function essential to the cell. To maintain the identity of each membrane-bound compartment, it is crucial that the trafficking of all cellular components be tightly regulated since a single mistake may lead to severe and undesirable outcomes

including cell death (Aridor and Hannan, 2000; Aridor and Hannan, 2002). Fortunately, the cell has several mechanisms to deal with various errors and thus allow cell activity to proceed as normal. One example is when newly synthesized proteins are packaged from the ER and taken to the Golgi for further post-translational modifications and/or sorting. Normally only the proteins destined for the secretory pathway are packaged into vesicles for transport, however, sometimes an ER-resident protein is accidentally loaded into the vesicle as well. To rectify this situation ER-resident proteins possess a sequence such as KDEL or KKXX at the C-terminus that mediates their return to the ER (Munro and Pelham, 1987; Nilsson et al., 1989). Through the use of signal-peptide sequences that mediate the localization of specific proteins to specific compartments, the cell is able to ensure the continued fidelity of intracellular trafficking.

However, sometimes defects go uncorrected by the cell. In the latter case the outcome varies depending on the type of error that occurred. When mutations are present in the coding sequence of a protein, sometimes the mutation may lead to the improper folding of the protein or may impair the function of the protein. In either case, the protein is unable to successfully perform its duty and the result is usually disease. In humans, there are many examples of mutations and/or loss of components of vesicular transport that are known to lead to disease. One example is Huntington's disease (HD), where HD is characterized by psychiatric problems, depression and hyperkinetic involuntary movements (Harper, 1996). This disease is caused by a mutation in the gene, IT15 which encodes a protein product called, huntingtin (Macdonald et al., 1993). The mutation affects gene transcription, protein-protein interactions, intracellular transport, neurotransmitter synthesis, release and neurotransmitter receptors. In HD patients a loss

of SNAP-25 (soluble *N*-ethylmaleimide-sensitive factor attachment protein receptor (SNARE) protein) and rabphillin 3a was reported (Smith et al., 2007), where the former is a Q-SNARE involved in fusion events at the plasma membrane (PM) and the latter is involved in vesicle docking and recycling, and where both proteins are crucial for neurotransmitter release. It is thought that a deficient pre-synaptic transmitter release due to loss of SNAP-25 and rabphillin 3a may explain some of the symptoms of HD. Another example is arthrogryposis-renal dysfunction-cholestasis (ARC) syndrome that is caused by a mutation in the VPS33B gene which subsequently leads to dysregulation of vesicle fusion (Gissen et al., 2004). These examples are only two of the many diseases that have been linked to defects in intracellular transport. Nonetheless, the message is clear that proper intracellular trafficking is crucial in maintaining optimal cellular conditions.

1.3 Tethers in Membrane Trafficking

There are many trafficking pathways within a eukaryotic cell (Whyte and Munro, 2002). Therefore, due to the abundance of trafficking pathways it is not impossible to imagine that each pathway contains its own set of players that impart the specificity of vesicle targeting and fusion to the acceptor membrane. As mentioned above, one of the first factors that determines the specificity of vesicle targeting are the tethers. In the eukaryotic cell, the tethers may be grouped into two different classes: long coiled-coil proteins and multi-subunit complexes.

To date, long coiled-coil proteins are known to be involved in Golgi and in endosomal fusion (Nielsen et al., 2000), however none have been associated with other transport steps. And because of their length which spans up to several times the diameter of a vesicle, it has been proposed that this class of tethers may be one of the first components to confer specificity to the targeting process by being anchored at one end to the acceptor membrane and using its other end to search the surrounding area for incoming vesicles (Lowe, 2000; Pfeffer, 1996; Waters and Hughson, 2000; Whyte and Munro, 2002). However, as of yet, there has been no direct evidence supporting this hypothesis. Some coiled-coil proteins are Uso1p in yeast which is required for the tethering of ER-derived vesicles to acceptor membranes (Barlowe, 1997), p115 which is the mammalian homologue of Uso1p and tethers COP I vesicles to the Golgi (Sonnichsen et al., 1998) and EEA1 which is required for the tethering of vesicles to the endosome (Dumas et al., 2001).

The second class of tethers consists of eight multi-subunit complexes that can be further divided into two distinct groups: three quatrefoil tethering complexes that are related to each other through a shared domain at the N-terminus (Whyte and Munro, 2002), and five non-quatrefoil tethering complexes that do not share any common domain. The three quatrefoil tethering complexes are the exocyst, *c*onserved *o*ligomeric *G*olgi (COG) and *G*olgi-*a*ssociated *r*etrograde *p*rotein (GARP), while the five non-quatrefoil tethering complexes are TRAPP I, TRAPP II, *ho*motypic fusion and vacuole *p*rotein *s*orting (HOPS), class *C co*re *v*acuole/*e*ndosome *t*ethering (CORVET) and Dsl1p (Whyte and Munro, 2002; Markgraf et al., 2007). In addition to sharing a common domain the former group also shares another similarity; each of the quatrefoil complexes

contains a multiple of four subunits which may reflect the ability to interact with a SNAREpin as tentatively proposed by Whyte and Munro (2002). And with regards to the entire class of multi-subunit complexes, structural similarity between subunits within a complex appears to be an emerging theme. In the exocyst, structural similarity between long α-helical rod structures of Exo70p and the C-terminal domains of Sec6p, Exo84p and Sec15 have been observed (Dong et al., 2005; Sivaram et al., 2006), and structural similarity between subunits has been speculated for the COG complex (Dong et al., 2005; Cavanaugh et al., 2007; Whyte and Munro, 2002). In the vertebrate TRAPP complex, the subunits can be grouped into two families: the bet3 family consisting of TRAPPC3, TRAPPC5 and TRAPPC6 and the sedlin family consisting of TRAPPC1, TRAPPC2 and TRAPPC4 (Sacher et al., 2008). At the structural level, along with the exocyst, TRAPP is one of the best studied multi-subunit tethering complexes to date and consequently is quickly becoming one of the complexes whose characterization is progressing steadily with time. It is now known that mutations in certain subunits of TRAPP lead to various trafficking disorders and sometimes disease (Chiari et al., 1999; Gedeon et al., 1999), hence insight into the molecular workings of TRAPP is critical in understanding its function.

1.3.1 TRAPP

Just over a decade ago, TRAPP (*Tra*nsport *P*rotein *P*article) was discovered as a novel and highly conserved tethering complex reported to participate in protein secretion (Sacher et al., 1998). Initial studies on TRAPP revealed the complex to be approximately 800 kDa in size and through fluorescence localization and subcellular fractionation studies, TRAPP was found to localize to the *cis*-Golgi. Subsequent work showed that the 800 kDa complex was one member of a pair of large complexes and was therefore called TRAPP II. A smaller and highly-related complex was found and called TRAPP I. While TRAPP II participates in membrane trafficking at a late Golgi compartment (Sacher et al., 2001; Cai et al., 2005), TRAPP I was found to mediate ER-to-Golgi transport (Sacher et al., 1998; Sacher et al., 2001).

The discovery of the TRAPP complexes came about through an immunoprecipitation study that was performed in order to gain insight into the function of the protein product of the *BET3* gene. A mutant in the *BET3* allele was identified in a yeast genetic screen as synthetically lethal with a *bet1* mutation, the latter being a gene whose protein product acts in ER-to-Golgi transport (Rossi et al., 1995). Using a radiolabelled yeast cell lysate containing *c-myc*-tagged Bet3p, Bet3p and its interacting partners were pulled down using an antibody directed against the *c-myc* tag. The corresponding sodium dodecyl sulphate – polyacrylamide gel electrophoresis (SDS-PAGE) revealed that nine other protein products precipitated with *c-myc*-Bet3p, and through the use of mass spectrometry the protein products were identified. The proteins are referred to as Trs20p, Trs23p, Trs33p, Bet5p, Trs31p, Trs85p, Trs65p, Trs120p and

Trs130p (Sacher et al., 1998; Sacher et al., 2000). While the first seven subunits are found in both TRAPP complexes, the latter three are unique to the TRAPP II complex (Sacher et al., 2001).

Table 1.1: Nomenclature of yeast and mammalian TRAPP subunits

Yeast open reading frames (ORFs)	Yeast TRAPP subunit (size in KD)	Mammalian TRAPP subunit (size in KD)	Aliases
YML077W	Bet5p (18)	TRAPPC1 (17)	MUM-2
YBR254C	Trs20p (20)	TRAPPC2 (16)	Sedlin
YKR068C	Bet3p (22)	TRAPPC3 (20)	
YDR246W	Trs23p (23)	TRAPPC4 (24)	Synbindin
YDR472W	Trs31p (31)	TRAPPC5 (21)	
YOR115C	Trs33p (33)	TRAPPC6a,b (18)	
YGR166W	Trs65p (65)	None	
YDR108W	Trs85p (85)	None	
YDR407C	Trs120p (120)	TRAPPC9 (140)	NIBP
YMR218C	Trs130p (130)	TRAPPC10 (142)	TMEM-1

Note: The above table is adapted from Sacher et al., 2008.

1.3.1.1 Assembly and Structure of TRAPP I

Since the discovery of TRAPP much research and insight has been gained concerning the structure and function of TRAPP and TRAPP subunits. Recently, the structure of the yeast *S. cerevisiae* and mammalian TRAPP I was solved. In both cases TRAPP I has an elongated, flat architecture with dimensions of ~180 Å x 65 Å x 50 Å (length x width x height) (Kim et al., 2006; Cai et al., 2008). Recombinant yeast and mammalian TRAPP I subcomplexes have been produced in *Escherichia coli* (*E. coli*). In yeast, recombinantly-expressed subunits of TRAPP I spontaneously form one stable complex where the tetrameric subcomplex: Bet3p-Trs33p-Bet5p-Trs23p is linked to the trimeric subcomplex: Bet3p-Trs31p-Trs20p. The two subcomplexes are linked through an interaction between Trs23p and Bet3p-Trs31p. An analogous recombinant mammalian TRAPP I complex did not assemble into one stable complex, rather the two stable subcomplexes mentioned above remain separate. Currently it is not known why the mammalian subcomplexes do not assemble into one complex as observed for the yeast proteins. However, it has been suggested that perhaps mammalian TRAPP I requires an as yet unidentified subunit to join the two subcomplexes together, or that a posttranslational modification is required for assembly (Kim et al., 2006; Sacher et al., 2008).

Nevertheless, despite the inability of the recombinant mammalian proteins to form one stable complex, the architecture of mammalian TRAPP I was elucidated by docking the crystal structures of the two mammalian subcomplexes into the electron microscopic (EM) density map of the yeast complex (Kim et al., 2006). Because the

crystal structure of the mammalian subcomplexes fit nicely into the density map of the yeast complex, the observed elongated flat structure of the TRAPP I complex is thought to be a conserved feature.

1.3.1.2 First Model of TRAPP I as a Tether

Early studies on the TRAPP I complex lead to the hypothesis that TRAPP I functions in the trafficking between the ER and the Golgi (Sacher et al., 1998). Today this hypothesis has been further characterized and supported by several groups (Sacher et al., 1998; Sacher et al., 2001; Jiang et al., 1998; Rossi et al., 1995), and it has been found that TRAPP I functions as a tethering factor for vesicles travelling from the ER to the Golgi.

Recently, two models have been proposed for TRAPP I mediated-vesicle tethering. In the first model (Kim et al., 2006) one of the first tethering interactions occurs by long, extended coiled-coil proteins such as p115 and/or GM130/golgin-95 in mammalian cells and by Uso1p in yeast. Once the vesicle is tethered, the coiled-coil proteins undergo a bending motion which brings the ER-derived vesicle closer to the Golgi where the vesicle can interact with another tethering factor, TRAPP I. In this model TRAPP I lies flat on the Golgi and lengthwise which means that 180 Å x 65 Å of TRAPP I is exposed for interaction with the incoming vesicle. This would also mean that the vesicle is now approximately 50 Å away from the Golgi and is thus within range for

SNAREpin formation. Fusion is then driven by the formation of a stable SNAREpin structure allowing for the release of the vesicle contents.

1.3.1.3 Second Model of TRAPP as a Tether

The second model is similar to the first, differing only in the way that TRAPP I is proposed to be oriented on the Golgi and/or acceptor membrane (Cai et al., 2008). In the second model TRAPP I is proposed to project lengthwise from the acceptor membrane. In this position it would interact with both the donor and acceptor membrane via conserved residues in the Bet3 subunit. Like the first model, this model is also plausible because it has been shown that TRAPP I mediates homotypic tethering between two COP II coated vesicles (Yu et al., 2006), and because Bet3p interacts with the Sec23p subunit of the COP II vesicle coat (Cai et al., 2007).

In both models, the common theme is that several factors are required in the docking of a vesicle to the acceptor membrane. The presence of several factors is necessary to ensure specificity because some factors such as GM130/golgin-95 are involved in processes elsewhere in the cell (Moyer et al., 2001). However, the main difference between the two models is that the first attempts to explain heterotypic fusion while the second attempts to explain both hetero- and homotypic fusion. In mammalian cells, both models are equally possible since both types of fusion events have been observed. However, in yeast cells homotypic fusion has not been reported. It has been

suggested that both models are not mutually exclusive but instead reflect the need of the complex to mediate two different types of fusion events (Sacher et al., 2008).

1.4 TRAPP as a Guanine Nucleotide Exchange Factor (GEF)

Another interesting feature of TRAPP – and perhaps connected to the tethering ability of the complexes – is the fact that both TRAPP complexes have GEF activity. GEFs are important because they stimulate the activation of specific Rabs by promoting the exchange of guanosine diphosphate (GDP) for guanosine triphosphate (GTP), which subsequently allows the activated Rab to regulate specific pathways within the cell. In the vesicular pathway between the ER and the Golgi, and after the tethering of the vesicle to the acceptor membrane, the activated form of the Rab, Ypt1p is believed to recruit downstream effector molecules which then promote the fusion of donor and acceptor membranes (Kim et al., 2006). Previous work has shown that TRAPP I is a GEF for Ypt1p while TRAPP II is a GEF for Ypt31/32p (Wang et al., 2000; Jones et al., 2000).

1.4.1 TRAPP I: GEF for Ypt1p

The TRAPP I core subunits required for GEF activity were elucidated to be two copies of Bet3p (Bet3-A and Bet3-B), Bet5p, Trs23p and Trs31p (Kim et al., 2006). More recently, the structure of the core subunits in complex with Ypt1p was solved (Cai

et al., 2008) which provided insight into the GEF activity of TRAPP I. It was observed that of the five core subunits only four subunits directly interacted with Ypt1p: Trs23p, Bet5p and the two copies of Bet3p. However, although Trs31p does not directly interact with the surface of Ypt1p, it is thought to be important in the formation and maintenance of the Ypt1p-TRAPP I interface (Cai et al., 2008). Furthermore, the crystal structure revealed that the C-terminus of the Bet3p-A protein occupies a similar position as the guanine nucleotide. This latter observation was noted by Cai et al. (2008) and suggests that the C-terminus of the Bet3p-A is responsible for initiating the exchange of GDP for GTP by inserting into the GTP-binding pocket of Ypt1p and acting as a wedge to initiate the conformational change required for GDP release. Although the latter model is certainly attractive, the fact that deletion of the C-terminus of Bet3p does not lead to a growth defect in yeast suggests refinement of this model is necessary. Therefore, further work remains to clarify whether the C-terminus of the Bet3p-A subunit is responsible for activating Ypt1p, and whether TRAPP I activates Ypt1p through an alternate method.

1.4.2 TRAPP II: GEF for Ypt31/32p

Compared to TRAPP I less is known about the GEF activity of TRAPP II at the structural level. Furthermore, it remains a controversial subject because various groups have shown results that appear to contradict each other. One piece of evidence that supports TRAPP II as a GEF for Ypt31/32p is that when Trs120p and/or Trs130p (both TRAPP II specific subunits) is mutated, Ypt31/32p GEF activity is abolished while

Ypt1p GEF activity is increased (Morozova et al., 2006). Conversely, another group has shown that TRAPP II is not a GEF for Ypt32p, but rather is a GEF for Ypt1p (Wang et al., 2000; Wang and Ferro-Novick, 2002). It has been suggested that these contradictory results may be a reflection of the different preparation methods used by each group (Sacher et al., 2008). However, what the surrounding controversy does make clear is that further work is required to resolve the current dispute surrounding the GEF activity of TRAPP II.

1.5 Sedlin

The TRAPP complexes have seven subunits in common, one of which is a protein called sedlin. In mammalian cells sedlin is also known as TRAPPC2, while in yeast cells sedlin's orthogue is called Trs20p. Sedlin is a small protein of 140 amino acids (aa) and sits at the extremity of the TRAPP complex where it is thought to participate in multiple protein-protein interactions. A connection between membrane traffic and skeletal development was revealed when it was found that patients with the disorder *S*pondylo*e*piphyseal *d*ysplasia *t*arda (SEDT) all had mutations in the gene encoding for sedlin (Gedeon et al., 1999). Currently, very little is known about the role(s) and function(s) of sedlin, however, several functions have been suggested in light of its presence in the TRAPP complex and its involvement in SEDT (Jang et al., 2002b; Kim et al., 2006). Additionally, sedlin has also been implicated in gene regulation after it was identified to be an interacting partner of *c-myc* promoter-binding protein 1 (MBP-1),

where MBP-1 is a protein that binds to the *c-myc* promoter and represses promoter activity (Ghosh et al., 2001).

1.5.1 Role of Sedlin in ER-to-Golgi Trafficking

As previously mentioned, sedlin is part of a large multi-subunit tethering complex called TRAPP. Within this complex, sedlin sits at one end where it may participate in multiple protein-protein interactions. Currently, the function(s) of sedlin is not known, however, sedlin is not required for the GEF activity of TRAPP (Kim et al., 2006). Therefore, what could be the function of sedlin in the TRAPP complex? It was suggested that sedlin may possess a regulatory and/or an adaptor role in trafficking between the ER and the Golgi by interacting with neighbouring SNAREs, since the crystal structure revealed that despite a lack of sequence similarity, sedlin is structurally similar to the N-terminal domain of two SNARE proteins, Ykt6p and Sec22p (Jang et al., 2002b). Furthermore, it was noted that the three proteins possess a common hydrophobic surface between α1 and β3. In Ykt6p this surface participates in the formation of the closed conformation, where the latter conformation prevents the association of R- and Q-SNAREs from forming the core complex which occurs prior to membrane fusion (Tochio et al., 2001), while in Sec22p the hydrophobic surface is involved in crystal-packing interactions (Gonzalez, Jr. et al., 2001). Additionally, sedlin was also found to possess many solvent-exposed apolar residues which is an unusual property for a protein. However, this unusual property suggests the fact that sedlin may participate in multiple

protein-protein interactions (Jang et al., 2002b), and some of these residues were indeed subsequently found to participate in interactions with other known TRAPP subunits (Kim et al., 2006).

1.5.2 Mutations in sedlin lead to *S*pondyloepiphyseal *d*ysplasia *t*arda (SEDT)

To date, greater than 30 different mutations in sedlin have been documented that cause SEDT (Savarirayan et al., 2003; Gecz et al., 2003), where SEDT is an X-linked recessive disorder whose onset occurs around the ages of ~10 – 15 years. SEDT affects the spinal vertebral bodies and epiphyses during skeletal growth and as a result affected individuals possess a short trunk and are of short stature (MacKenzie et al., 1996). Although this disorder is not life-threatening it is nonetheless debilitating since affected individuals develop premature arthritis predominantly in the spine and hip joints, and in the third decade of life usually require surgery to reduce joint pain (Taybi and Lachman, 1996). Currently, there is no specific treatment for SEDT, however healthy eating, maintaining a healthy weight-for-height, and regular low-impact exercise such as swimming or cycling is advised (Savarirayan et al., 2003).

Although there have been a variety of documented mutations in the gene encoding for sedlin that lead to SEDT no correlation has yet been found between the location of the mutation and the observed effect on the phenotype as all mutations lead to the appearance of SEDT with no varying degree in the severity of the symptoms (Gedeon et al., 2001). However, in yeast, various mutations in the sedlin gene exhibit subtle differences. Some

mutations known to cause SEDT in humans were able to complement a *TRS20* disruption while others could not (Gedeon et al., 2001). The latter observation was explained in two ways. Either in humans the clinical differences between each individual are so subtle that they escape detection, or the functions of sedlin and Trs20p are different in metazoan and non-metazoan eukaryotes. The fact that human sedlin can compensate for Trs20p (Gecz et al., 2003) suggests that perhaps sedlin and Trs20p share some overlapping and/or similar function(s).

Thus far it is clear that mutations in the sedlin gene cause SEDT, however the molecular mechanism of how SEDT develops remains to be elucidated. Currently several scenarios have been suggested. One possibility is that sedlin mutations impede proper collagen secretion and thus normal bone growth is affected. Another possibility is that sedlin has a function independent of the trafficking pathway and disruptions in this independent function lead to SEDT (Sacher, 2003). Therefore by studying sedlin/Trs20p and sedlin-related proteins insight into the function and role of sedlin may be gained.

1.5.3 Sedlin pseudogenes and sedlin-related proteins

The fact that SEDT is an X-linked recessive disorder not only indicates the genetic nature of the disorder but it also reveals the fact that only one functional copy of sedlin is sufficient to suppress the SEDT phenotype. This fact is supported through the observation that female carriers do not display the SEDT phenotype. The latter observation brings up an interesting issue because if one copy of sedlin is sufficient to

carry out the function(s) of sedlin, then what happens when the protein product of an open reading frame (ORF) identical to the sedlin gene and sedlin-related genes comes into the picture? More precisely the question is, can the latter protein products contribute and/or fulfill the role(s) and function(s) of sedlin? Since sedlin has one retropseudogene and one sedlin-related protein, by answering the latter question insight may be gained concerning the function(s) and role(s) of sedlin.

In the human genome there are a total of seven pseudogenes. However, out of the seven, one is a retropseudogene: C2.19 (also known as SEDLP1) located on chromosome 19 (Gecz et al., 2000). The retropseudogene C2.19 is interesting because it contains an ORF identical to the sedlin ORF. Moreover, it is intriguing that C2.19 has been shown to be transcribed and potentially translated (Ghosh et al., 2001; Scrivens et al., 2009), which could potentially allow the protein product of C2.19 to compensate for a lack of sedlin in the cell. As well, tissue-specific expression of C2.19 may also explain why SEDT is tissue specific and why there is a lack of severe growth defects in SEDT patients.

Most recently a sedlin-related protein was identified and is called, TRAPPC2L (TRAPPC2-like and will be herein referred to as C2L) (Scrivens et al., 2009). This protein was found through a Basic Local Alignment Search Tool (BLAST) using the yeast Trs20p as the query and is 27% identical to Trs20p and 28% identical to sedlin. Interestingly, like sedlin, C2L interacts with the TRAPP complex as shown by size exclusion chromatography using mammalian cell lysates (Scrivens et al., 2009). C2L does not appear to replace sedlin in the complex, rather it has been proposed that C2L sits at the opposite extremity of the complex compared to sedlin (Figure 1.1). Whether C2L may compensate for a lack of sedlin in the cell has yet to be shown, however the fact that

the D47 residue (known to cause SEDT when changed to tyrosine) is conserved from sedlin to C2L may suggest a conserved function. On the other hand, phylogenetic analysis revealed that sedlin and C2L occur in pairs across species which suggests a conserved functional divergence. Further supporting a functional divergence, it has been shown that C2L is unable to compensate for a loss of Trs20p in yeast (Scrivens et al., 2009). Nonetheless, C2L may compensate for a lack of sedlin since C2L is a sedlin-related gene exhibiting 28% identity to sedlin. Further work remains to be done to shed light on this matter.

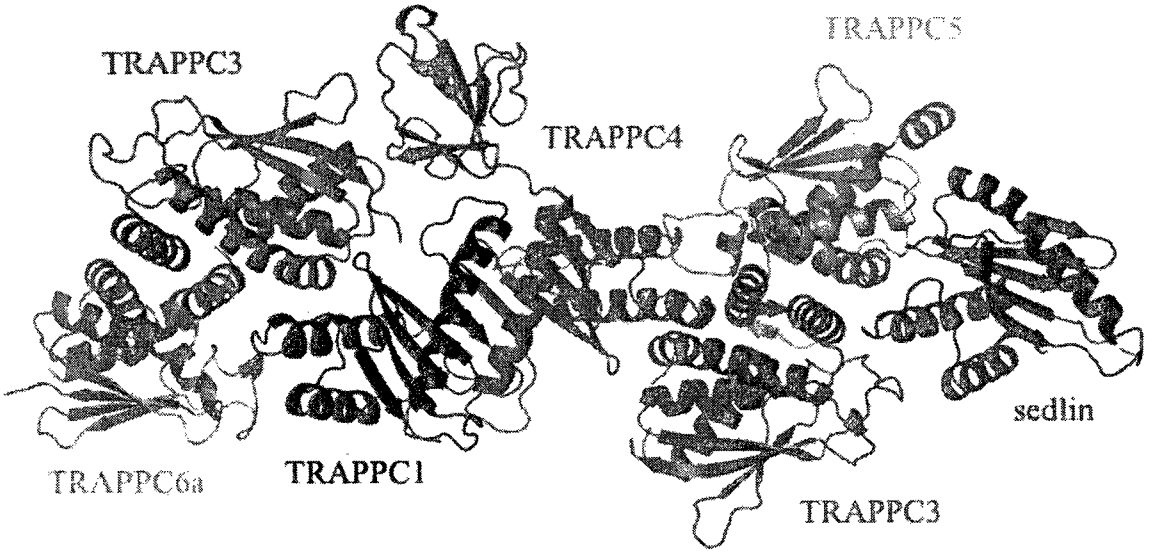

Note: The above image is adapted from (Sacher et al., 2008).

Figure 1.1: Mammalian TRAPP. TRAPP consists of seven subunits as seen above. Within the complex sedlin sits at one extremity while the novel TRAPP interactor, C2L, is believed to sit at the opposite extremity. Note that C2L is not shown above.

1.5.4 Sedlin and Other Possible Functions

In addition to a role in membrane trafficking and a role in SEDT, sedlin has been suggested to have a role in gene regulation. As mentioned above, sedlin was found to interact with a protein called MBP-1 that binds to the *c-myc* promoter and represses promoter activity which in turn leads to apoptosis (Ghosh et al., 2001). The binding of sedlin to MBP-1 was found to relieve the repression caused by MBP-1 and thus decrease apoptosis. In a follow-up study (Ghosh et al., 2003) it was found that expression of sedlin was able to repress luteinizing hormone β (LHβ) promoter activity, where regulated LHβ expression is crucial for reproduction (Tremblay and Drouin, 1999). In the latter study, the regulation of the LHβ gene was studied because sedlin was found to be expressed predominantly in systems related to reproduction such as testis and pituitary, and other tissues such as the right cerebellum and adrenal glands (Ghosh et al., 2003). Another study revealed sedlin was found to interact with chloride intracellular channel (CLIC1 and CLIC2) proteins (Fan et al., 2003). The latter proteins are thought to be involved in homeostasis of membrane potential, maintenance of intracellular pH and control of cell volume. Currently, the significance of the latter interaction is unknown however the apparent interaction between the respective proteins suggests sedlin may aid in one or more of the aforementioned functions of the CLIC proteins, or may recognize the CLIC proteins as cargo on a vesicle.

1.6 Project: A yeast two-hybrid screen identifies a novel interactor of the TRAPP subunit sedlin

As seen above, currently the function of sedlin is unknown. Nevertheless, sedlin has been implicated in trafficking between the ER and the Golgi due to its presence in the TRAPP complex and is implicated in the skeletal disorder, SEDT. In addition, sedlin may have a role in gene regulation as well as an as-yet undefined function within the cell. In this project I use a yeast two-hybrid screen (Y2H) to identify interacting partners of sedlin in order to further characterize and gain a deeper insight into its function.

1.6.1 Yeast two-hybrid (Y2H)

Developed in 1989 (Fields and Song, 1989), the Y2H screen remains one of the leading molecular tools to study protein-protein interactions in native intracellular conditions. This screen is not only inexpensive, but can also be carried out in almost any laboratory with results seen within a matter of days. In addition, compared to other methods used to study protein-protein interactions such as crosslinking and co-immunoprecipitation, the Y2H screen allows one to detect transient interactions that may not be normally detected in the former approaches. This innovative technology employs the GAL4 transcriptional activator and takes advantage of the fact that GAL4 can be physically separated into two domains whose function can be re-established once the two domains are brought into proximity. In the classic Y2H screen two fusion proteins are

required: a protein of interest fused to the DNA binding domain (BD) of GAL4 (also referred to as the bait protein) and the library protein(s) fused to the activation domain (AD) (also referred to as the prey protein). Interaction between the bait and prey protein brings the BD and AD of GAL4 close enough together to allow transcription of the downstream reporter genes that subsequently allows growth on selective media.

However, although the classic Y2H screen is an attractive method to study a protein there are also some limitations. One limitation is that although this screen occurs within yeast cells and thus occurs under native cellular conditions, the bait and prey protein must both be able to translocate to the nucleus in order to allow transcription of the reporter gene. Therefore, interactions between the bait protein and membrane-bound, integral membrane and/or proteins localized to subcellular compartments cannot be detected and would generate what is called a false negative. Further, the bait and prey protein should not be able to autoactivate the reporter gene which would lead to the appearance of false-positives. False positives are one of the biggest drawbacks of the Y2H screen because the appearance of false positives may occur for multiple reasons, such as the one just mentioned or non-specific interactions. However, these limitations can be overcome. If the bait or prey protein autoactivates the reporter gene(s) then by using increasing concentrations of 3-amino-1,2,4-triazole (3AT) the expression of the *HIS3* gene product (which is one of the reporter genes in the Y2H screen) is inhibited accordingly. To distinguish false positives from the real interactors, the identified interaction should be verified through other methods such as pull-down assays and coimmunoprecipitations. Finally, in order to overcome the generation of false negatives other Y2H systems have been developed: the *S*OS- and the *R*AS *r*ecruitment *s*ystems

(SRS and RRS) (Hubsman et al., 2001) which detects interactions with membrane-bound proteins and the Split-ubiquitin system (Stagljar et al., 1998) which detects interactions occurring between cytosolic proteins and membrane proteins.

2. Materials and Methods

2.1 Plasmid constructs, Oligonucleotides and Strains

For the Y2H screen, the bait construct (pGBKT7-sedlin) was made by amplifying mouse sedlin using the oligonucleotides sedlinFEcoRI and sedlinREcoRI (Table 2.1) followed by ligation into the bait vector, pGBKT7 (Clontech). Standard amplification mixture contained 1x polymerase buffer, 200 μM dNTP, ~30 ng template DNA, 500 nM forward oligonucleotide, 500 nM reverse oligonucleotide, 1.25 U of polymerase. The correct orientation was selected for following a digest with MscI where the expected fragment sizes were 4786, 2895 and 49 base pairs (bp) for the correct orientation and 4786, 2539 and 405 bp for the incorrect orientation. SPATA4 constructs were prepared by amplifying the ORF from mouse testis cDNA, which was a kind gift from Dr. James Scrivens from Concordia University, using the oligonucleotides SPATA4-F-HindIII, mSPATA4-R-BamHI, SPATA4-F-BamHI and mSPATA4-R-XhoI (Table 2.1). The amplified product of the two former and the two latter oligos respectively was ligated into pFLAGCMV6a (Sigma) and pMALc2X (New England Biolabs) respectively. To generate the pGBKT7-sedlin (APA) construct the QuikChange® protocol (Stratagene) was followed and oligonucleotides C2_APA_UP and C2_APA_DN were used to introduce the APA mutation into the template, pGBKT7-sedlin. All other oligonucleotides, strains and plasmid constructs used in this study can be found in Tables 2.1, 2.2 and 2.3 respectively. All bacterial strains were grown at 37°C for 16 hours, while

all yeast strains were grown at 30°C for 48 hours unless otherwise indicated. All liquid cultures were aerated at 250 rpm unless otherwise indicated.

Table 2.1: Oligonucleotides used in this study

Oligonucleotides	Sequence
sedlinFEcoRI	AGGAATTCATGTCTGGGAGCTTCTACTTC
sedlinREcoRI	AGGAATTCTTAGCTTAAAAGGTGTTTCTTC
SPATA4-F-BamHI	CGCGGATCCATGGCTGCCGCCGGCCAGG
mSPATA4-R-XhoI	TCAGCTCGAGTCACAGGTTTTCAGTGTTCTC
SPATA4-F-HindIII	CCCAAGCTTATGGCTGCCGCCGGCCAGG
mSPATA4-R-BamHI	CGCGGATCCTCACAGGTTTTCAGTGTTCTC
T7 sequencing primer	TAATACGACTCACTATAGGG
T7 terminator sequencing primer	GCTAGTTATTGCTCAGCGG
pGAD-F-ID	CTATTCGATGATGAAGATACCCCACCAAACCC
pGAD-R-ID	GTGAACTTGCGGGGTTTTTCAGTATCTACGATT
CMV24	TATTAGGACAAGGCTGGTGGGCAC
CMV30Seq	GTCGTAATAACCCCGCCCCGTTGACGC
SP6	TATTTAGGTGACACTATAG
pGEXseq	GATAAGTACTTGAAATCCAGC
C2_APA_UP	TATATAAAGTTTGCAATGGCTCCAGCTTATGAACCCAATTCTCCC
C2_APA_DN	GGGAGAATTGGGTTCATAAGCTGGAGCCATTGCAAACTTTATATA

Table 2.2: Strains used in this study

Strain	Genotype	Source
AH109	MATa, trp1-901, leu2-3, 112, ura3-52, his3-200, gal4Δ, gal80Δ, LYS2::GAL1UAS-GAL1TATA-HIS3, GAL2UAS-GAL2TATA-ADE2, URA3::MEL1UAS-MEL1TATA-lacZ	Clontech
Y187	MATα, ura3-52, his3-200,ade2-101, trp1-901, leu2-3, 112,gal4Δ, gal80Δ, met–, URA3 : : GAL1UAS-GAL1TATA-LacZ MEL1	Clontech

Table 2.3: Plasmid constructs used in this study

Plasmid Constructs	Fusion	Epitope	Yeast Selection	Bacterial Selection	Sources
pGBKT7	GAL4 BD	c-Myc	TRP1	kanamycin	Clontech
pGBKT7-sedlin	GAL4 BD-sedlin	c-Myc	TRP1	kanamycin	This study
pGBKT7-sedlin (D47Y)	GAL4 BD-sedlin (D47Y)	c-Myc	TRP1	kanamycin	This study
pGBKT7-sedlin (APA)	GAL4 BD-sedlin (APA)	c-Myc	TRP1	kanamycin	This study
pGBKT7-C2L	GAL4 BD-C2L	c-Myc	TRP1	kanamycin	This study
pGADT7RecAB	GAL4 AD	HA	LEU2	ampicillin	Clontech
pGADT7RecAB-hSPATA4	GAL4 AD-SPATA4	HA	LEU2	ampicillin	Clontech
pGADT7RecAB-hBet3	GAL4 AD-Bet3	HA	LEU2	ampicillin	Clontech

pGADT7RecAB-REPS2	GAL4 AD-REPS2	HA	LEU2	ampicillin	Clontech
pGADT7RecAB-POSTN	GAL4 AD-POSTN	HA	LEU2	ampicillin	Clontech
pGADT7RecAB-SPATA22	GAL4 AD-SPATA22	HA	LEU2	ampicillin	Clontech
pGADT7RecAB-LAP3	GAL4 AD-LAP3	HA	LEU2	ampicillin	Clontech
pGADT7RecAB-Neg	GAL4 AD-Neg	HA	LEU2	ampicillin	Clontech
pFLAGCMV6a	(N)FLAG	FLAG	-	ampicillin	Sigma
pFLAGCMV6a-mSPATA4	(N)FLAG-SPATA4	FLAG	-	ampicillin	This study
pRK5MYC	(N)Myc	Myc	-	ampicillin	Clontech
pRK5MYC-sedlin	(N)Myc-sedlin	Myc	-	ampicillin	N. Shahrzad
pMALc2X	(N)MBP	MBP	-	ampicillin	NEB
pMALc2X -mSPATA4	(N)MBP-SPATA4	MBP	-	ampicillin	A. Moores
pET15b-sedlin	(N)6xHis-sedlin	6xHis	-	ampicillin and chloramphenicol	Byung-Ha Oh
pRO EXTHa-mBet3 & pACYCDuet-1-hTrs31/sedlin	Bet3/hTrs31/sedlin-6xHis (C)	6xHis	-	ampicillin and chloramphenicol	N. Shahrzad
pCMV-(myc)3-ECT2	(N)Myc-ECT2	Myc	-	ampicillin	A. Piekny (Yuce et al., 2005)

BD: GAL4 binding domain; AD: GAL4 activation domain

2.2 Tissue Culture and preparation of cell lysates

Human embryonic kidney 293T (HEK 293T) cells were grown in Dulbecco's modified Eagle Medium (DMEM) supplemented with 10% fetal bovine serum (FBS, Wisent) and 1% penicillin/streptomycin (P/S).Cells were kept in a humidified 5% CO_2 chamber at 37°C. Transfections were carried out in either 10 (for coimmunoprecipitation) or 15 (for gel filtration) cm dishes with 10 or 20 µg of DNA, respectively, using the calcium phosphate method as described below (Section 2.2.1). Cells were harvested 48 hours post-transfection by scraping with 500 or 1,000 µl coimmunoprecipitation (CoIP) lysis buffer (1% Triton X-100, 1 mM EDTA, 50 mM Tris pH 7.5, 150 mM NaCl) with 1 mM sodium orthovanadate and protease inhibitor (Roche) for 10 or 15 cm dishes, respectively. For gel filtration, cells were collected as above using gel filtration lysis buffer (150 mM NaCl, 50 mM Tris pH 7.2, 0.5 mM EDTA, 1 mM DTT, 1% Triton X-100) with protease inhibitor (Roche). For western analysis 30 µg of lysate was used.

2.2.1 Calcium phosphate transfection

Cells were plated at ~50% confluence and grown in supplemented DMEM as indicated above (section 2.2). The following day, cells were transfected with 1 ml of transfection mixture (1x Hepes buffered saline (HBS; 25 mM HEPES, 0.75 mM Na_2HPO_4, 5 mM KCl, 140 mM NaCl, 6 mM dextrose), 10-20 µg DNA and 84 mM calcium chloride). The medium was replaced with fresh medium 24 hours post-

transfection. Cells were harvested 48 hours post-transfection as indicated above (section 2.2).

2.4 Yeast two-hybrid screen (Y2H)

2.4.1 Mating the bait with the prey strain

The Y2H screen was performed as described in the Matchmaker™ Pretransformed Libraries User Manual. Briefly, a 50 ml culture of the bait strain (AH109 containing pGBKT7-sedlin) was grown to an OD_{600} of 0.8-0.9 in –Trp medium and then centrifuged at 1,000 *g* for 5 minutes and resuspended in 5 ml of –Trp medium. Then, 1 ml of the prey strain (Pretransformed Normalized Matchmaker™ Human Universal cDNA Library in Y187 (Clontech)) was added and the total volume of the culture was brought to 50 ml using 2x YPDA (0.1% yeast extract, 0.2% peptone, 0.2% dextrose, 0.3% L-adenine hemisulphate). The cells were mated for 24-28 at 30°C hours with shaking at 50 rpm. Cells were subsequently plated on quadruple drop out (QDO; 0.67% yeast nitrogen base, 2% dextrose, 0.08% -Trp/-Leu/-His/-Ade dropout mix) solid medium containing X-α-Gal and left at 30°C for 3-8 days.

2.4.2 Analysis and Verification of putative positive clones

2.4.2.1 Retesting phenotypes

To ensure that each positive clone contained only one prey plasmid, positive clones were streaked on double drop out (DDO) (0.67% yeast nitrogen base, 2% dextrose, 0.08% -Trp/-Leu dropout mix) solid medium containing X-α-Gal. One clone from the latter plate was then picked and streaked onto triple drop out (TDO) (0.67% yeast nitrogen base, 2% dextrose, 0.08% -Trp/-Leu/-His dropout mix) solid medium containing X-α-Gal to verify that the phenotype was maintained. If a clone contained more than one prey plasmid then a mixture of blue and white colonies would result after streaking.

2.4.2.2 Colony polymerase chain reaction (PCR)

Positive clones were picked and inserts in pGADT7 were amplified via polymerase chain reaction (PCR) using oligonucleotides pGAD-F-ID and pGAD-R-ID. The conditions for PCR consisted of: 1 cycle of 94°C for 3 minutes, followed by 30 cycles of 94 seconds for 30 seconds, 68 °C for 3 minutes, 72 °C for 7 minutes, ending with an elongation step of 72 °C for 7 minutes. The identity of the amplified products was determined by DNA sequencing.

2.4.2.3 Rescuing plasmid DNA from yeast and bacterial transformations

Plasmids were rescued from yeast cells as described in the adapted protocol by Michael Jones based on the QIAprep® Spin Miniprep Kit protocol (Michael Jones, Chugai Institute for Molecular Medicine, Ibaraki, Japan). The adapted version employed acid washed glass beads (Sigma) to mechanically lyse the yeast cells after resuspension in resuspension buffer (Fermentas). Purification of the plasmid proceeded as per the manufacturer's instructions. Following the rescue of the plasmid from the yeast cells, the plasmid was transformed into electrocompetent DH5α bacterial cells to amplify the plasmid. Transformations were done using 0.5-2 µl of DNA in 40 µl of electrocompetent cells. Cells were briefly shocked in a sterile 2mm electroporation cuvette and grown in 1 ml of SOC (2% tryptone, 0.5% yeast extract, 10 mM NaCl, 2.5 mM KCl, 10 mM $MgCl_2$, 10 mM $MgSO_4$, 20 mM Glucose) at 37°C for 1 hour, followed by plating on solid luria-Bertani medium (LB) (0.5% yeast extract, 1% tryptone, 1% NaCl) containing the appropriate antibiotic.

2.4.2.4 High efficiency yeast transformations

High efficiency yeast transformations were done as described by Gietz and Woods (2002). Briefly, 50 ml cultures were grown to an OD_{600} of 2.0 and made competent after washing with sterile water and resuspension in an appropriate volume of transformation master mix (33.3% polyethylene glycol 3500, 100 mM lithium acetate,

1.4 µg/µl boiled single-stranded-carrier DNA). Cells were then incubated in a 42°C water bath for 40 minutes. Prior to plating, cells were pelleted by centrifugation at 13,200 rpm for 30 seconds in a table top microcentrifuge and pellets resuspended in either 0.5 or 1 ml of sterile water. Cells were plated on the appropriate selective solid medium and incubated at 30°C for 2-4 days.

2.5 Coimmunoprecipitation using HEK 293T cell lysates

HEK 293T cells were co-transfected as above (section 2.2.1) with pRK5MYC-sedlin and pFLAGCMV6a-SPATA4 constructs and the appropriate controls. CoIP samples contained 1 mg of lysate (prepared as in section 2.2) made up to a total volume of 1 ml with 1x phosphate buffered saline (PBS; 8% NaCl, 0.2% KCl, 1.44% Na_2HPO_4, 0.24% KH_2PO_4). Immunoprecipitation was done with 2 µg of rabbit anti-myc IgG(Abcam) on ice, at 4°C for 16 hours, followed by incubation with 10 µl of Protein A-agarose (Bioshop), on a nutator at 4°C for 2 hours. Samples were then washed 3x with 1 ml 1x PBS with spinning in a refrigerated microcentrifuge for 30 seconds at 5,000 rpm. Finally, 25 µl of 1x sample buffer (SB) (62.5 mM Tris-HCl pH 6.8, 2% SDS, 7.5% Glycerol, 0.005% Bromophenol Blue, 2.5% β-mercaptoethanol (Bioshop)) was added to samples, heated at 95°C for 2 minutes and either stored at -20°C or loaded on a SDS-PAGE gel for Western analysis. Western blotting was done as indicated below (section 2.5.1). For Western analysis of the CoIP samples, primary antibodies used were monoclonal mouse anti-myc (Upstate) and monoclonal mouse anti-FLAG (Sigma) both

at 1:5,000 dilution. Secondary antibody used was affinity purified peroxidase-labelled goat anti-mouse IgG (anti-mouse; Kirkegaard & Perry Laboratories) at 1:10,000 dilution.

2.5.1 SDS-PAGE and Western blotting

Samples were electrophoresed in 1x running buffer (1.44% glycine, 0.303% Tris and 1% SDS), at 150 volts until the loading dye reached ~1 cm from the bottom of the gel. Samples were then transferred onto a polyvinylidenefluoride (PVDF) membrane (Millipore) in transfer buffer (0.303% Tris, 1.44% glycine, 20% methanol) at 100 volts for 1 hour using a Biorad Mini-Gel apparatus. Membrane was then stained with Ponceau stain (0.1% Ponceau Red in 5% glacial acetic acid) for 5 minutes and molecular weight standards were marked with pencil. The Ponceau stain was then removed by washing the membrane twice in PBS containing 0.2% Tween (PBSt; 8% NaCl, 0.2% KCl, 1.44% Na_2HPO_4, 0.24% KH_2PO_4, 0.2% Tween (Amresco)), 10 minutes per wash. Blocking was done for 1 hour using blocking solution (5% skim milk prepared in 1x PBSt). Incubation with primary and secondary antibodies occurred for 1 hour. The membrane was then exposed using either 1 ml of enhanced chemiluminescent (ECL) western blotting detection reagents (GE Healthcare), or to detect weaker signals 500 µl of high sensitivity chemiluminescent substrate (Millipore). Between incubation steps, the membrane was washed twice with PBSt as above. All antibodies were diluted in blocking solution and all incubations were done at room temperature (RT) with gentle shaking.

2.6 Gel Filtration

HEK 293T cells were co-transfected as above (section 2.2.1) with pRK5MYC-sedlin and pFLAGCMV6a-SPATA4 constructs and the appropriate controls. Cells were prepared and lysed as indicated above (section 2.2). Samples contained 5 mg of lysate made up to a total volume of 1 ml with gel filtration buffer (150 mM NaCl, 50 mM Tris pH 7.2, 0.5 mM EDTA, 1 mM DTT) and was loaded on a Superdex^{TM} 200 column (GE Healthcare), where the flow rate was 0.5 ml/min and 0.5 ml fractions were collected. After fractionation, 25 µl of each sample was loaded on a SDS-PAGE gel for Western analysis. Western blotting was done as above (section 2.5.1). Western analysis for gel filtration employed mouse anti-myc (Sigma) and mouse anti-FLAG antibody (Upstate) simultaneously at 1:5,000 dilution, followed by anti-mouse at 1:10,000 dilution. Membrane was exposed as above (section 2.5.1).

2.7 Purification of Recombinant proteins and *in vitro* Binding Assay

2.7.1 Purification of MBP- and His-tagged proteins

To purify MBP-tagged proteins a modified protocol for purifying soluble fusion proteins by New England Biolabs was used (pMAL Protein Fusion & Purification System – Instruction Manual). Cells were grown to an OD_{600} of 0.5-1.0 at 37°C and protein production was induced by the addition of 1 mM IPTG with shaking at 250 rpm at 25°C

overnight. Cells were then pelleted at 4,000 rpm for 20 minutes at 4°C in the Avanti-J251 centrifuge (Beckman Coulter TM). Cell pellets were then resuspended in 25 ml of column buffer (20 mM Tris-HCl, 200 mM NaCl, 1 mM EDTA, 1 mM DTT) and either frozen at -80°C for future use, or were immediately sonicated for 2 minutes by a series of non-consecutive 10 second pulses. Lysates were then clarified at 20,000 *g* for 20 minutes at 4°C and the supernatant (crude extract) collected. The crude extract was then diluted 1:6 with column buffer and then poured onto a disposable 1.5 x 12 cm column (Biorad) containing a bed volume of 500 µl of amylose resin (New England Biolabs) pre-equilibrated with column buffer. Retained proteins were washed with 5 column volumes of column buffer before being eluted with 11 ml of elution buffer (20 mM Tris-HCl, 200 mM NaCl, 1 mM EDTA, 1 mM DTT, 10 mM maltose (Bioshop)) in 1 ml fractions. Protein concentration was then assayed using the Biorad Protein Assay dye-reagent as per manufacturer's instructions. Concentrated protein samples were then pooled together and passed through a 10 DG column (Biorad) in 1x binding buffer (10 mM HEPES pH 7.4, 25 mM NaCl, 115 mM KCl, 2 mM $MgCl_2$, 0.1% Triton X-100) to remove excess maltose and the protein concentration was redetermined as above.

To purify His-tagged proteins, cells were grown and induced as indicated above. Cells were pelleted at 4,000 rpm for 30 minutes at 4°C in the Avanti-J251 centrifuge (Beckman Coulter TM). Pellets were then resuspended in 35 ml of lysis buffer for His-tagged proteins (300 mM NaCl, 50 mM Tris-HCl pH 8.5, 9.7 mM β-mercaptanol, 0.5% Glycerol, 0.1% Triton X-100, 1 mM AEBSF) and sonicated as above. Cell lysates were then centrifuged at 30,000 *g* for 30 minutes and crude extract was collected. The crude extract was then incubated at 4°C on a nutator with 1 ml of Ni-NTA Agarose (Qiagen) to

allow binding, and then passed through a 1.5 x 12 cm disposable column. The retained proteins were then washed twice with 10 ml wash buffer (50 mM Tris-HCl pH 8.5, 300 mM NaCl, 10 mM β-mercaptanol) before being eluted with 3 ml of imidazole elution buffer (50 mM Tris pH 8.8, 200 mM NaCl, 200 mM imidazole) in 1 ml fractions. Protein concentration was then assayed as above.

2.7.2 *In vitro* Binding Assay

In vitro binding assays contained 0.1 μM of either MBP or MBP-SPATA4 with increasing amounts (0, 0.05, 0.1, 0.25 μM) of a heterotrimeric complex composed of His-sedlin/TRAPPC3/TRAPPC5 or 0.5 μM of either MBP or MBP-SPATA4 with increasing amounts (0, 0.1, 0.2, 0.5 μM) of N-terminal 6xHis-tagged sedlin (His-sedlin). Note that i*n vitro* binding assays containing the heterotrimeric complex were also performed using the latter concentrations, however, using the former concentrations allowed for better visualization of increased binding of sedlin to SPATA4. Samples were made up to a total volume of 250 μl with 1x binding buffer and left on ice at 4°C for 1 hour to allow binding. Pulldown employed 10 μl amylose resin (New England Biolabs) on nutator for 1 hour. Samples were washed 3x with 250 μl of 1x binding buffer, and spun down for 30 seconds at 5,000 rpm. Protein was eluted from the beads by heating to 95°C in 25 μl of 1x SB for 2 minutes prior to storage at -20°C or loading on a SDS-PAGE gel for Western analysis. Western blotting was performed as above (section 2.5.1). Western analysis used affinity purified, polyclonal antibody recognizing sedlin (anti-sedlin) at a dilution of

1:10,000. The secondary antibody used was affinity purified antibody peroxidase-labelled goat anti-rabbit IgG (anti-rabbit) at 1:10,000 dilution (anti-rabbit; Kirkegaard & Perry Laboratories). Membrane was exposed as above (section 2.5.1).

3. Results

3.1 Identification of sedlin interactors using the classic Yeast two-hybrid screen

To study sedlin the Matchmaker™ GAL4 Two-Hybrid System 3 (Clontech), which is a classic Y2H screen was employed to look for novel interactors of the protein. This approach was taken because the Y2H is a simple, fast and effective way to determine novel protein-interactors, which therefore allows for the elucidation of the function(s) and role(s) of sedlin by knowing the function(s) and role(s) of its interacting partner(s). The principle behind the Y2H is that two fusion proteins are created that contain either the BD of the GAL4 transcriptional activator (termed the bait protein), or the AD of GAL4 (termed the prey protein). When an interaction takes place, GAL4 transcriptional activity is reconstituted as measured by the production of the reporter genes *HIS3, ADE2, MEL1* and *lacZ* which allow the production of histidine, adenine, α-galactosidase and β-galactosidase respectively (Figure 3.1).

In this Y2H screen the bait protein contained sedlin fused to the BD (pGBKT7-sedlin) while the prey proteins were a library of pretransformed human cDNA in the AD vector (Clontech). Before the screen was conducted, it was necessary to ensure that the bait protein did not autoactivate the reporter genes. Therefore, approximately 100 cells of the strain AH109 containing pGBKT7-sedlin were plated on –Trp/-His solid medium containing varying concentrations of 3AT (3AT prevents the production of histidine by inhibiting the His3 protein), where the concentration ranged from 0 – 60 mM 3AT. By

repeating this procedure three times it was found that 0.5 mM of 3AT was necessary to remove any autoactivation of the reporter genes caused by sedlin (Figure 3.2). However, 1 mM of 3AT was used in the actual screen to ensure that autoactivation did not occur. After mating the library to the query strain (pGBKT7-sedlin) cells were plated on –Trp/-Leu/-His/-Ade (QDO) solid medium containing X-α-gal, where X-α-gal is a substrate for α-galactosidase and allows the production of a blue coloration for white/blue screening. The Y2H screen resulted in hundreds of hits, where the resulting colonies were of various sizes and varying shades of blue. However, since only the strong interactors of sedlin were desired only the dark blue colonies were picked for further analysis. This resulted in 184 colonies being selected.

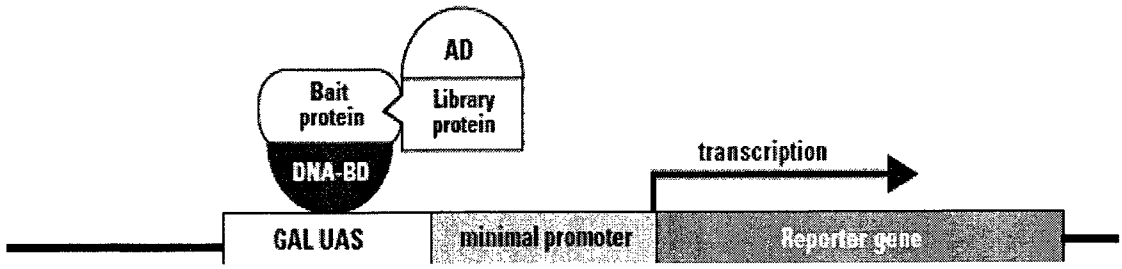

Note: The above image was taken from the Matchmaker™ Pretransformed Libraries User Manual.

Figure 3.1: Principle of the Y2H screen. In the classic Y2H screen two fusion proteins are expressed separately, where one fusion protein is fused to the binding domain (BD) of the GAL4 transcriptional activator and is called the bait protein while the other is fused to the activation domain (AD) of GAL4 and is called the prey protein (or the library protein). Only when the bait and the prey protein physically interact can the transcription of the reporter genes be activated, which subsequently allows growth on the selective dropout solid media –Trp/-Leu/-His (TDO) and –Trp/-Leu/-His/-Ade (QDO).

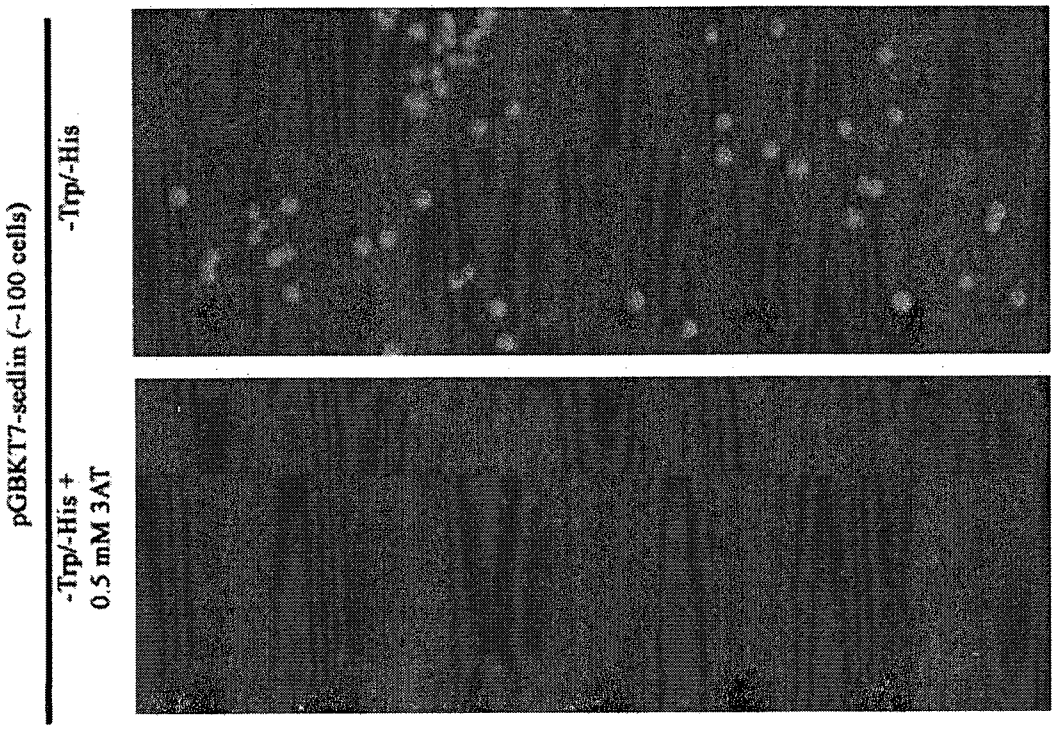

Figure 3.2: Autoactivation by sedlin is inhibited by 0.5 mM 3AT. Before the Y2H screen was performed it was found that sedlin (the bait protein) autoactivates the reporter genes. Therefore, to correct for the autoactivation, ~100 cells of the strain AH109 containing pGBKT7-sedlin was plated on several –Trp/-His solid medium containing various concentrations of 3AT ranging from 0 - 60 mM 3AT. It was found that 0.5 mM 3AT was the minimum concentration needed to inhibit the autoactivation. The top panel shows the autoactivation caused by sedlin when the strain AH109 containing pGBKT7-sedlin is plated on –Trp/-His solid medium without 3AT, while the bottom panel shows that in the presence of 0.5 mM 3AT the autoactivation is inhibited as observed by the appearance of pinpoint colonies.

3.2 Analysis of interactors reveals SPATA4 as a novel interactor of sedlin

To begin analyzing the potential sedlin interactors, it was necessary to make sure that each positive isolate contained only one prey plasmid. If a clone contained more than one prey plasmid then further analysis on the clone would likely result in confusing data. Therefore, each clone was first streaked on DDO solid medium containing X-α-gal, followed by choosing one blue colony and streaking on TDO solid medium containing X-α-gal. After both streakings a mixture of blue and white colonies was not observed which indicated that each positive clone contained only one prey plasmid. Next, colony PCR was performed on each clone to confirm that each prey plasmid contained an insert. The latter result showed that the majority of clones did contain an insert since an intense band of a specific size was observed for all successful amplifications (data not shown). For the unsuccessful amplifications the PCR was repeated with success (measured as a single band from the PCR reaction) for all but five colonies. However, although the five clones did not give an amplification product, it is unlikely that an insert is not present since the clones are able to grow on DDO and TDO solid medium which indicates that an interaction between the bait and prey protein is present. Most likely the five clones that were unamplified require very specific amplification settings that were not met in the general settings used for the rest of the clones.

In an attempt to detect the presence of inserts represented multiple times in the screen, and thus obtain a reliable estimation for the number of sedlin interactors obtained using the Y2H screen, an *AluI* digest was performed on the amplified products. *AluI* was chosen as the restriction enzyme since it is known to be a frequent cutter recognizing the

sequence AGCT. From the resulting digestion patterns (data not shown), inserts were grouped together and were thought to represent identical inserts. However, after sequencing it was discovered that not all inserts within a group represented the same insert. This mistake most likely arose due to human error, since the digestion patterns were analyzed by eye and thus subtle differences in the digestion patterns of unique inserts may have escaped notice. Nonetheless, this method removed 15 duplicates from the list of sedlin interactors and thus 169 hits remained for further analysis (Table 3.1).

As the former approach was unable to give a reliable estimation of the number of unique sedlin interactors that were obtained from the Y2H, prey plasmids were rescued from the positive clones and retransformed into an AH109 strain containing either pGBKT7-sedlin or pGBKT7, where the former transformation served to reconfirm the interaction between sedlin and its interacting partner and the latter served as a control and allowed for the removal of false-positives (prey proteins that autoactivate the reporter genes). Thus, the rescue and subsequent transformation of prey plasmids narrowed down the list of sedlin interactors and allowed for only reconfirmed sedlin interactors to be sent for sequencing. The transformation of prey plasmids was also done in an AH109 strain containing pGBKT7-TRAPPC2L since C2L is a sedlin-like protein and is hypothesized to functionally compensate for mutated sedlin in SEDT patients (Scrivens et al., 2009). Therefore, it was of interest to see whether proteins that interacted with sedlin also interacted with C2L. The transformation of prey plasmids into the strain AH109 containing pGBKT7-sedlin was performed for all hits, however only 53 transformations were successful. The inability to transform the remaining 116 prey plasmids is thought to be due to an unsuccessful rescue of the corresponding prey plasmids from the original

colonies. Of the 53 transformations, 34 were observed not to interact with sedlin, 10 were false positives, while 9 were reconfirmed as sedlin interactors. It is unknown why some of the hits were not reconfirmed. Sequencing of the 9 sedlin interactors revealed that 2 were contigs while 1 was out of frame (presumably resulting in a non-specific interaction), leaving 6 sedlin interactors (Table 3.2 and Figure 3.3). Of the 6 sedlin interactors, one was found to be TRAPPC3 which was previously identified as a sedlin interactor (Kim et al., 2006). This latter result increases the confidence in the 6 reconfirmed sedlin interactors.

To better characterize the function(s) and role(s) of sedlin, efforts were focused on one novel sedlin interactor called SPATA4. We decided to characterize the interaction between sedlin and SPATA4 since SPATA4 was found to interact with sedlin but not with C2L. This observation was interesting because thus far, all the proteins that interacted with sedlin also interacted with C2L. Therefore, this indicates that the interaction of SPATA4 with sedlin is specific and suggests that sedlin contains at least one unique function that cannot be carried out by C2L.

Table 3.1: Sequenced prey inserts obtained from sedlin Y2H screen

Clone No.	Gene	Accession Number	No. of Clones
10	CDC7 - homo sapiens cell division cycle 7 homolog	NM_003503.2	1
13	_- - Homo sapiens chromosome 10 genomic contig, alternate assembly	NW_001838014.1	1
30	PRKRIR (DAP4; P52rIPK; MGC102750) - protein-kinase, interferon-inducible double stranded RNA dependent inhibitor, repressor of (P58 repressor)	NM_004705.2	1
34	NEK2 - NIMA (Never in mitosis gene a) - related kinase 2	NM_002497.2	1
40	_-- Homo sapiens chromosome 8, clone RP11-713M15	AC104958.6	1
42 (47)	SELL - homo sapiens selectin L (Lymphocyte adhesion molecule 1)	NM_000655.3	2
44	FKBP3 - FKBP3 binding protein 3, 25 kDa	NM_002013.2	1
50	REPS2 (POB1; REPS2) - RALBP1 associated Eps domain containing 2	NM_001980975.1	1
59	POLR2G - polymerase (RNA) II (DNA directed) polypeptide	NM_002696.1	1
60 (67)	PTGER3 - Prostaglandin E. receptor 3 (subtype EP3)	NM_198719.1	2
63	_- - Homo sapiens chromosome 12 genomic contig, alternate assembly	NW_001838063.1	1
64 (112, 113)	POSTN - periostin, osteoblast specific factor	NM_006475.1	3
69 (111)	SPATA22 - spermatogenesis associated 22	NM_032598.3	2
78	ALDH1A1 (ALDC; ALDH1; PUMB1; ALDH11; RALDH1; ALDH-E1; MGC2318; ALDH1A1) - aldehyde dehydrogenase 1 family,	NM_000689.3	1

	member A1		
79	HS6 - homosapiens chromosome 6 genomic contig, alternate assembly	NW_001838990.2	1
82	_- - Homo sapiens chromosome 7 genomic contig, reference assembly	NT_007819.16	1
83	ARID2 - AT rich interactive domain 2 (ARID, RFX-like)	NM_152641.2	1
88 (12)	SPATA4 - spermatogenesis associated 4	NM_144644.2	2
89 (90)	POLR3H - polymerase (RNA) III (DNA directed)	NM_138338.2	2
93 (15, 29, 167, 175, 153)	ZNF350 - zinc finger protein 350	NM_021632.3	6
94	TRAPPC3 - homo sapiens trafficking protein particle complex 3	NM_014408.3	1
95	FOXN3 - forkhead box N3	NM_001085471.1	1
102 (33)	LRRTM3 - leucine rich repeat transmembrane neuronal 3	NM_178011.3	2
108 (107)	NSL1 - NSL1, MIND kinetochore complex component, homolog	NM_015471.3	2
130	LAP3 - Homo sapiens leucine aminopeptidase 3, mRNA	NM_015907.2	1
140	MYC - v-myc myelocytomatosis viral oncogene homolog	NM_002467.3	1
142	FAM47E - family with sequence similarity 47, member E (Homo sapiens similar to genethonin 1, transcript variant)	XM_001720938.1	1
143 (79)	HS6 - homosapiens chromosome 6 genomic contig, reference assembly	NT_007299.12	1
144	NRBF2 - Homo sapiens nuclear receptor binding factor	NM_030759.3	1

	2 (mRNA)		
146	ASXL1 - additional sex combs like 1 (Drosophila)	NM_015338.4	1
148	DLGAP5 - homo sapiens discs, large homolog 7 (Alias: HURP)	NM_014750.3	1
154	SPOP - speckle-type POZ protein	NM_003563.3	1
162	NUP155 - nucleoporin 155 kDa	NM_153485.1	1

Note: In total there are 184 clones obtained from the Y2H screen, however only the sequenced colonies were included in the table.

Table 3.1: Sequenced prey inserts obtained from sedlin Y2H screen. In an attempt to estimate the number of unique interactors obtained from the sedlin Y2H screen all 184 hits were amplified and subsequently digested with *AluI*. Similar digestion patterns were then grouped together and were assumed to represent the same insert. Sequencing of a few groups revealed that within a group not all inserts were identical. This table provides a complete list of all the sequenced inserts along with their corresponding accession number. The corresponding clone number is also provided, where clone numbers within parenthesis indicate clones containing identical inserts.

Table 3.2: Summary of Potential Interactors, False Positives and Non-Interactors of Sedlin

Clone No.	Gene	Accession Number
Potential Interactors		
130	LAP3 - Homo sapiens leucine aminopeptidase 3, mRNA	NM_015907.2
50	REPS2 (POB1; REPS2) - RALBP1 associated Eps domain containing 2	NM_001980975.1
64 (112, 113)	POSTN - periostin, osteoblast specific factor	NM_006475.1
69 (111)	SPATA22 - spermatogenesis associated 22	NM_032598.3
88 (12)	SPATA4 - spermatogenesis associated 4	NM_144644.2
94	TRAPPC3 - homo sapiens trafficking protein particle complex 3	NM_014408.3
63	*_ - - Homo sapiens chromosome 12 genomic contig, alternate assembly*	*NW_001838063.1*
82	*_ - - Homo sapiens chromosome 7 genomic contig, reference assembly*	*NT_007819.16*
78	*ALDH1A1 (ALDC; ALDH1; PUMB1; ALDH11; RALDH1; ALDH-E1; MGC2318; ALDH1A1) - aldehyde dehydrogenase 1 family, member A1*	*NM_000689.3*
False Positives		
30	PRKRIR (DAP4; P52rIPK; MGC102750) - protein-kinase, interferon-inducible double stranded RNA dependent inhibitor, repressor of (P58 repressor)	NM_004705.2
93 (15, 29, 167, 175, 153)	ZNF350 - zinc finger protein 350	NM_021632.3
102 (33)	LRRTM3 - leucine rich repeat transmembrane neuronal 3	NM_178011.3
55, 98, 110, 114, 125, 144, 152		
Non-Interactors		
13	_ - - Homo sapiens chromosome 10 genomic contig, alternate assembly	NW_001838014.1

5, 6, 11, 14, 16, 18, 19, 20, 22, 24, 26, 28, 31, 35, 36, 39, 45, 56, 58, 65, 68, 73, 77, 80, 81, 92, 99, 101, 104, 105, 117, 127, 149		

Table 3.2: Summary of Potential Interactors, False Positives and Non-Interactors of Sedlin. Prey plasmids were rescued from positive clones and transformed into the yeast strain AH109 containing either pGBKT7-sedlin or pGBKT7, where the former transformation serves to reconfirm the interaction with sedlin and the latter serves to remove false positives (prey proteins that autoactivate the reporter genes). Cells were plated on DDO solid medium to confirm the presence of the bait and prey plasmids and were also plated on TDO solid medium containing 1 mM 3AT to detect the interaction between the bait and prey proteins. The above table classifies the results of the transformations as either containing a potential interactor if the interaction was reconfirmed, false positive if the prey protein autoactivates the reporter genes or non-interactor of sedlin if the interaction was not reconfirmed. Out of 53 successful transformations, 9 were classified as potential interactors, 10 as false positives and 34 as non-interactors of sedlin. Subsequent to the sequencing of the 9 potential interactors a total of 3 hits were disqualified since 2 inserts were contigs while the remaining insert was out of frame. The hits that were removed as potential interactors are indicated in *italicized* font.

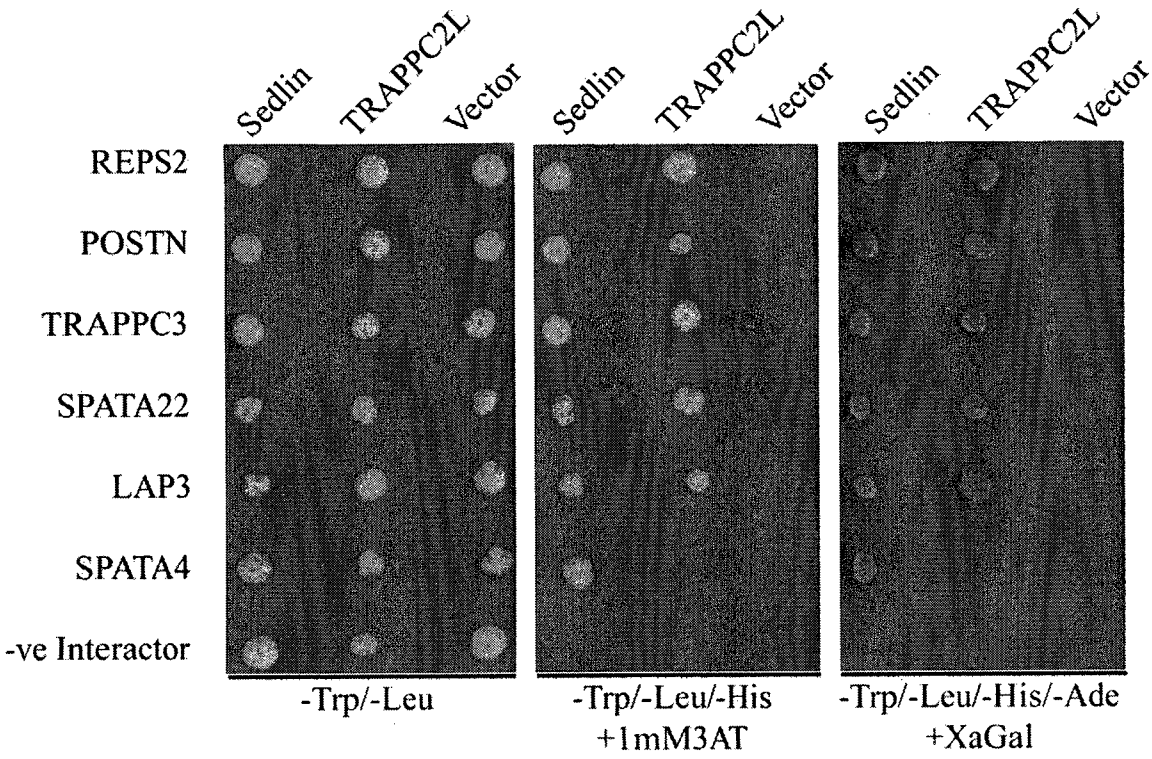

Figure 3.3: Sedlin interactors obtained from Y2H screen. Prey plasmids were rescued from positive clones and transformed into the yeast strain AH109 containing either pGBKT7-sedlin, pGBKT7-TRAPPC2L or pGBKT7. Cells were grown to an OD_{600} of 1.0 and plated on DDO, TDO and QDO solid medium to show respectively, the presence of both plasmids and the interaction between the bait and prey protein under medium and high stringency conditions. The TDO and QDO solid medium both reveal that SPATA4 interacts with sedlin but not with C2L. The negative interactor is clone 149 from the Y2H screen, however the identity is not known since it was not sent for sequencing.

3.3 Bioinformatic analysis of SPATA4

To ensure that the SPATA4 Y2H insert accurately represents SPATA4, the prey vector, pGADT7-SPATA4, was sequenced. Sequencing revealed the presence of a few mutations within the nucleotide sequence (Figure 3.4A) and consequently within the peptide sequence of SPATA4 (Figure 3.4B). In the nucleotide sequence, a silent mutation, an insertion mutation resulting in a frameshift, and a deletion mutation shortly thereafter were detected. The protein sequence of SPATA4 was observed to be nearly identical to the actual SPATA4 sequence with the exception of the presence of short peptide sequences at the beginning and the end of the translated protein, where the former is due to translation of the 5' untranslated region while the latter is due to the frame shift mutation. Furthermore, the frame shift causes a premature termination of the SPATA4 protein and results in the absence of 38 residues from the C-terminus. These results suggest that the extreme carboxy-terminus of SPATA4 is not involved in its interaction with sedlin.

SPATA4 is a relatively novel protein and as such not much is known concerning the cellular function(s) that SPATA4 may play. To characterize SPATA4 a bioinformatics analysis was performed. A phylogenetic tree of SPATA4 across thirteen different species (Figure 3.5A) reveals that SPATA4 from *Homo sapiens* is more closely conserved in orthologues from primates and more divergent when compared to orthologues found in aquatic species and *Gallus gallas* (chicken). The latter observation is better seen in Table 3.3 where the percent identity of SPATA4 across the thirteen different species is given. The table also reveals that among species, SPATA4 ranges

from 39-99% identity which indicates a fairly high degree of conservation throughout evolution, and moreover suggests a conserved importance for SPATA4. A multiple sequence alignment of SPATA4 from eight different species was also performed (Figure 3.5B). The alignment revealed that the majority of conserved residues are in the middle of the protein sequence which, as determined by Conserved Domains (NCBI) is where a domain of unknown function (DUF1042) is located. The DUF1042 domain of SPATA4 spans from residues 55-211. In an attempt to learn more about SPATA4 and the DUF1042 domain, a BLAST search within the human genome was performed using the DUF1042 sequence from SPATA4 as the query. The search found two proteins called SPEF1 and SPEF2 (sperm flagellar 1 and 2, respectively). Interestingly, the latter proteins are also implicated in spermatogenesis (Chan S.W. et al., 2005; Sironen et al., 2006). A multiple sequence alignment of the three DUF1042 domains revealed fourteen identically conserved residues that lay within a calponin homology (CH) domain as determined by Conserved Domains (NCBI) (Figure 3.5C).

In an effort to examine the expression profile of SPATA4 Genecards (http://www.genecards.org) was used. While an electronic Northern (Figure 3.5D middle panel) and the literature on SPATA4 suggest a testis-specific expression pattern, microarray data (Figure 3.5D top panel) suggests a broader expression pattern.

A

*gggggg*ccgcagcaacccagaaagcgtcatggctgccgccggccaggaaaaagggtatttgacacagactgcggcagccc
tagacaagtcaccgtcactttcgccacagctagcagctcccatccgagggaggcctaagaagtgtctggtctatccgcatgcgc
cgaagagctcccgcttgtctcgttccgttctgcgttggcttcagggtctggatctcagcttcttccccaggaacatcaacagagattt
ttcaaatggcttcctaattgcagaaatattctgtatatattacccctgggaacttgaattatcatcctttgaaaacgggacctctttaaaa
gtcaagttggataactgggcacagttggagaagttcctggcaagaaaaaaatttaaattacctaaagaactaatccatggaacaat
tcattgtaaagctggagtgcctgaaatattgatagaagaggtttacactttattaacacatcgagaaattaaaagtatccaggatgac
tttgtgaatttcacggactatagctaccagatgcgtttacccctggtttccaggtctacagtttcgaagtctattaaagataacattagg
ttatcagaattactaagcaatcccaacatgctgaccaatgaacttaaagcggagttcctcatccttttacatatgttgcaaagaaaatt
aggcagaaaattgaatccggaatggtttgatgtgaaaccaacagtgggagaagttactctcaatcaccttcctgcccaagcctctg
ggcgcagatataatttaaaagttaaaagaggaagagttgtccctgtttt**a**ccaaatataggtagtggtggcagttcacatagagaa
atacatgtgaagcaagctgacaacattcttattactctgctatgaaacctatcagaaacatggacaagaaaccttgaaaagcacct
gtcaaatggctttgaagaagtgatgccaccatctctagccataataaagaaacagaatcacctagtattggatgtatttcaataataa
atagagtggtgtcttttccacaaaaaaaaaaaaaaaaaaa

B

GGRSNPFSVMAAAGQEKGYLTQTAAALDKSPSLSPQLAAPIRGRPKKCLVYPHA
PKSSRLSRSVLRWLQGLDLSFFPRNINRDFSNGFLIAEIFCIYYPWELELSSFENGT
SLKVKLDNWAQLEKFLARKKFKLPKELIHGTIHCKAGVPEILIEEVYTLLTHREIK
SIQDDFVNFTDYSYQMRLPLVSRSTVSKSIKDNIRLSELLSNPNMLTNELKAEFLIL
LHMLQRKLGRKLNPEWFDVKPTVGEVTLNHLPAQASGRRYNLKVKRGRVVPV**T**
TKYR

Figure 3.4: Sequence analysis of SPATA4 from Y2H library. A) Nucleotide sequence of SPATA4 insert from Pretransformed Normalized Matchmatker™ Human Universal cDNA Library. Sequencing of the prey vector, pGADT7-SPATA4, revealed the presence of a few mutations in the nucleotide sequence of SPATA4. Highlighted in purple is a silent mutation of A to G, highlighted in red is the insertion of a T and subsequently a frame shift for downstream codons, highlighted in blue indicates the deletion of a G nucleotide immediately following the highlighted nucleotide and subsequently indicates the end of the frame shift. *Italicized* nucleotides indicate the extra

G's added to the insert by the reverse transcriptase used to make the library, the blue font is the sequence corresponding to the coding sequence (CDS) of SPATA4, and the black font at the beginning and end of the sequence correspond to the 5' and 3' untranslated regions, respectively. **B) Protein sequence of SPATA4 insert from Pretransformed Normalized Matchmaker™ Human Universal cDNA Library.** Blue font corresponds to residues identical to the protein sequence of SPATA4. Highlighted in red are residues that are not part of the SPATA4 protein: the first highlighted portion corresponds to the translation of the 5' untranslated region, while the second highlighted portion corresponds to the frame shift caused by the insertion of a T nucleotide. Also note that the insertion causes the premature termination of the SPATA4 protein, where the above SPATA4 protein is missing 38 residues at the C-terminus.

A

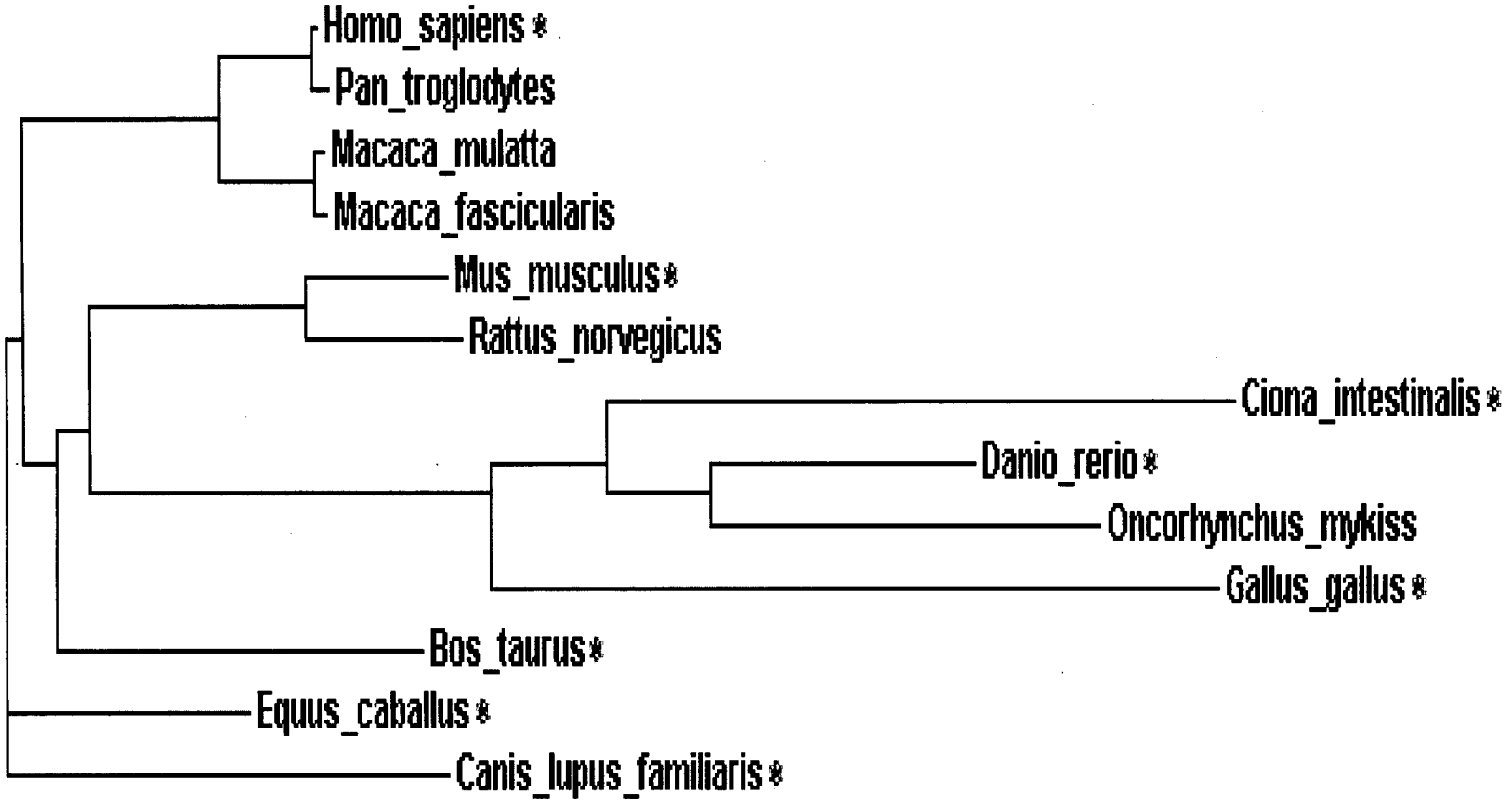
Homo_sapiens
Pan_troglodytes
Macaca_mulatta
Macaca_fascicularis
Mus_musculus
Rattus_norvegicus
Ciona_intestinalis
Danio_rerio
Oncorhynchus_mykiss
Gallus_gallus
Bos_taurus
Equus_caballus
Canis_lupus_familiaris

B

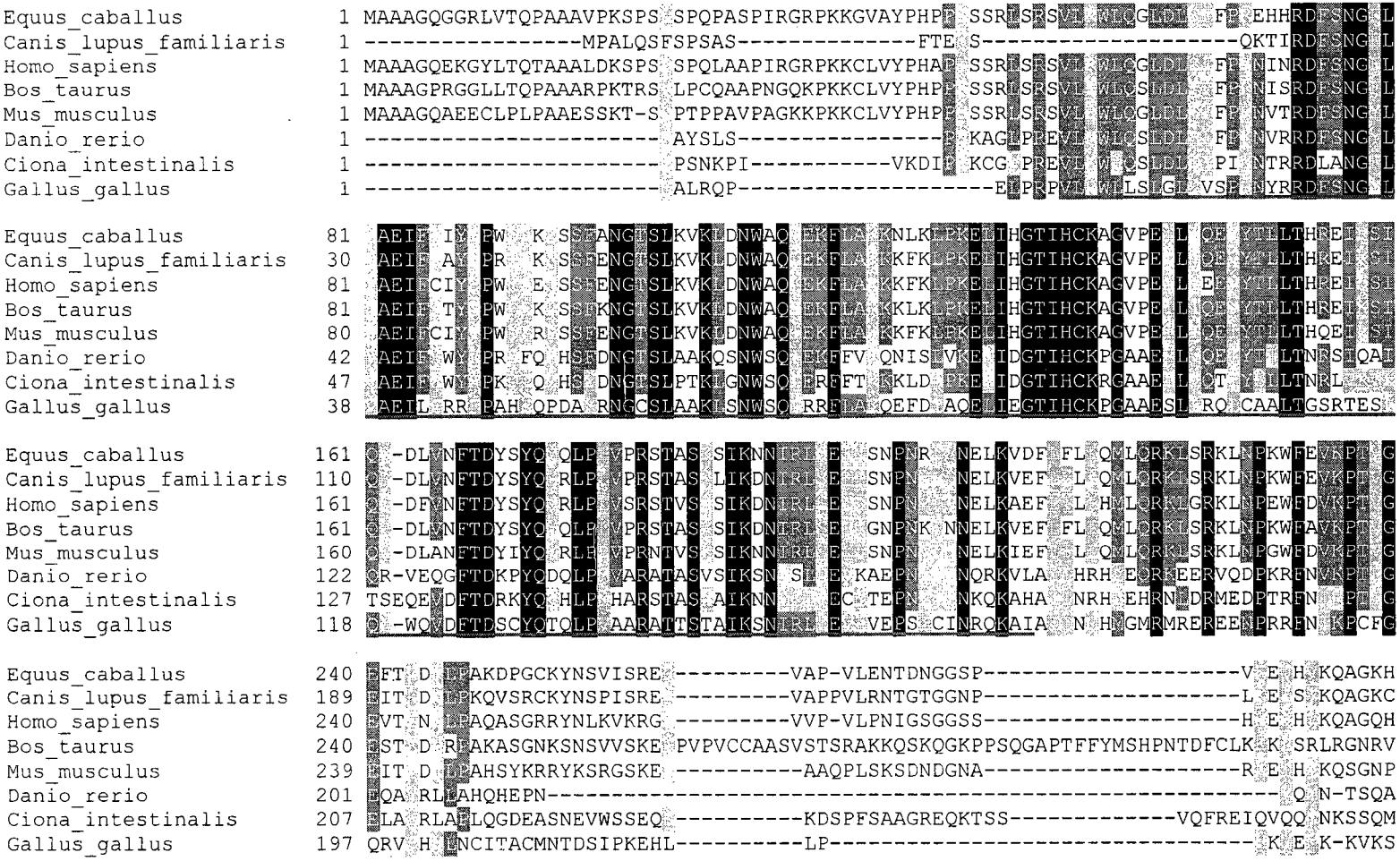
Equus_caballus
Canis_lupus_familiaris
Homo_sapiens
Bos_taurus
Mus_musculus
Danio_rerio
Ciona_intestinalis
Gallus_gallus

```
Equus_caballus           290 SLESIRKPIRN------------MKK-------
Canis_lupus_familiaris   240 SFESEIYQKQGKVTLESTRLMA-LKK-------
Homo_sapiens             290 SYYSAMKPIRN------------MDKKP-----
Bos_taurus               320 STPKEIEVKQTRTYSDCMKPTINVEKEPEEAPV
Mus_musculus             289 CENTENL--------------------------
Danio_rerio              223 AC-------------------------------
Ciona_intestinalis       264 SVKPGSIHTIQ-TPVFTQ---------------
Gallus_gallus            233 SVNCGSFSSETGAAALTL---------------
```

C

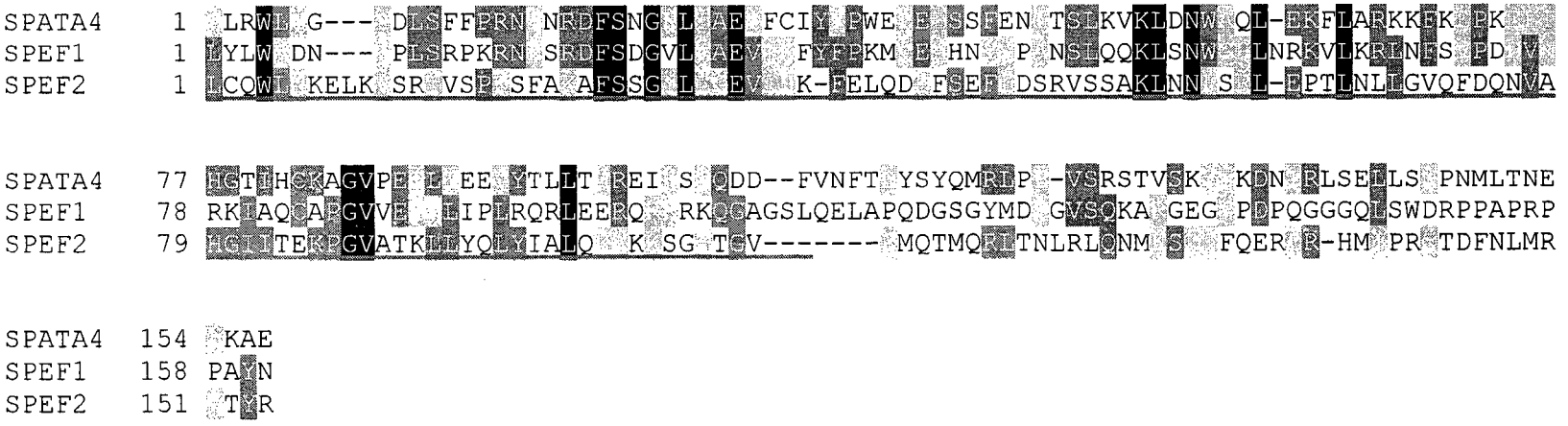

D

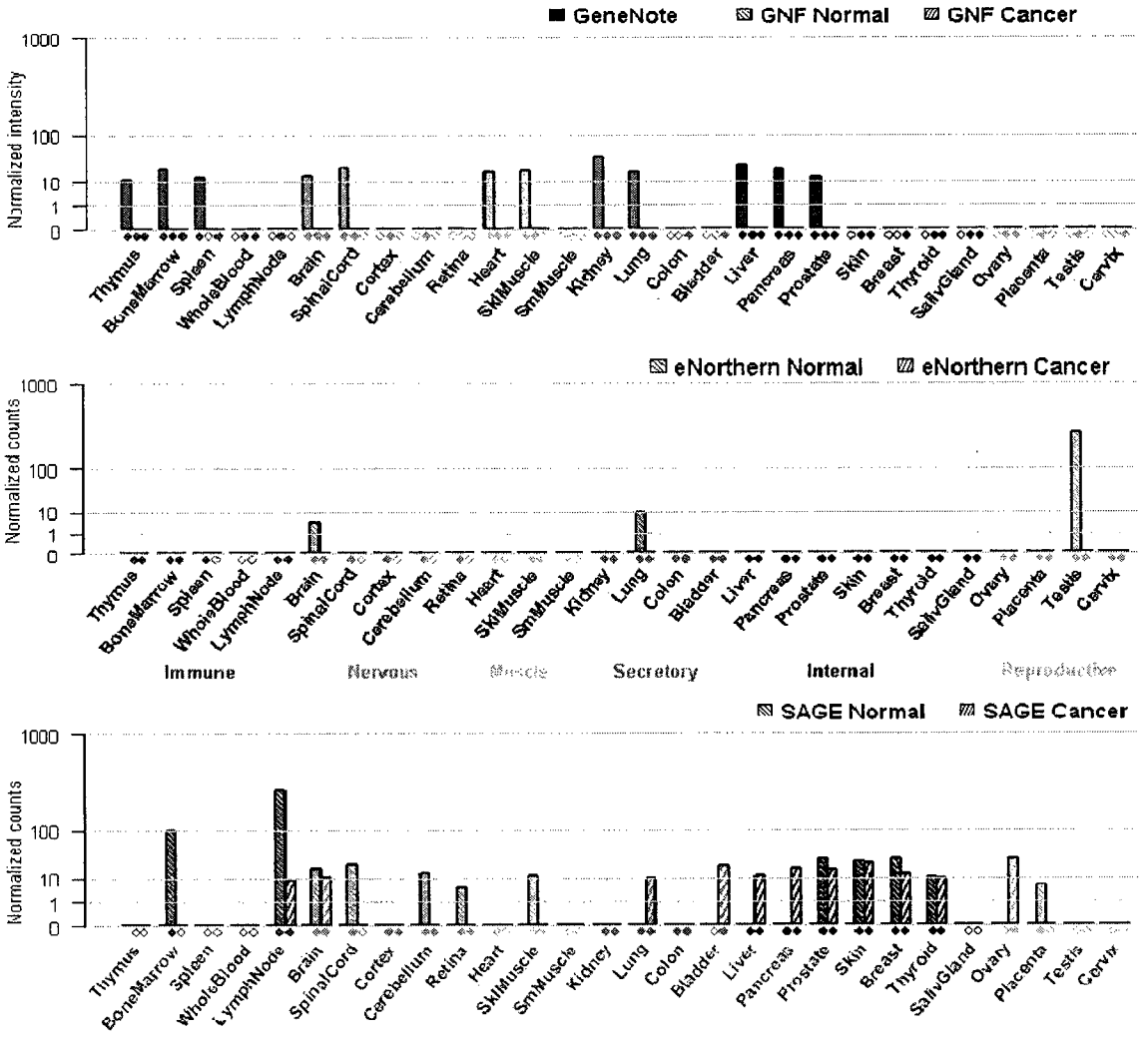
GeneNote
GNF Normal
GNF Cancer
Normalized intensity
1000
100
10
1
0
Thymus
BoneMarrow
Spleen
WholeBlood
LymphNode
Brain
SpinalCord
Cortex
Cerebellum
Retina
Heart
SkMuscle
SmMuscle
Kidney
Lung
Colon
Bladder
Liver
Pancreas
Prostate
Skin
Breast
Thyroid
SalivGland
Ovary
Placenta
Testis
Cervix
eNorthern Normal
eNorthern Cancer
Normalized counts
Immune
Nervous
Muscle
Secretory
Internal
Reproductive
SAGE Normal
SAGE Cancer

Figure 3.5: Bioinformatic analysis of SPATA4 (Homo sapiens). A) Phylogenetic tree of SPATA4. The phylogenetic tree for SPATA4 was made using the free software program ClustalW and contains thirteen SPATA4 homologues. The accession numbers are: *Bos Taurus*: NP_001011677.1; *Canis lupus familiaris*: XP_851298; *Ciona intestinalis*: NP_001029005.1; *Danio rerio*: NP_001004013.1; *Equus caballus*: XP_001493059; *Gallus gallus*: NP_001026309.1; *Homo sapiens*: NP_653245.2; *Macaca fascicularis*: BAE01027.1; *Macaca mulatta*: NP_001030604.1; *Mus musculus*: NP_598472.2; *Oncorhynchus mykiss*: NP_001117998.1; *Pan troglodytes*: NP_001008990.1; *Rattus norvegicus*: NP_001002852.1. The asterisk indicates the species used in the multiple sequence alignment (B) of SPATA4. **B) Multiple sequence alignment of SPATA4.** A multiple sequence alignment of eight of the thirteen SPATA4 homologues was performed using ClustalW and conserved residues were highlighted using Boxshade. The black, dark grey and light grey shading represent residues that display 100% identity, at least 70% identity and at least 70% similarity, respectively. The underlined region indicates the position of the DUF1042 domain which spans from residue 55-211 in *Homo sapiens*. Note that eight sequences were used in the multiple alignment as only one representative sequence was taken from each order of organisms. Also note that the selection of the representative sequence for the various orders was randomly selected. **C) Mulitple sequence alignment of the DUF1042 domain of SPATA4, SPEF1 and SPEF2.** Analysis of *Homo sapiens* DUF1042 domains from three proteins by ClustalW and Boxshade (as performed above) revealed the presence of 14 residues that display 100% identity, which are indicated by black shading. The dark grey and the light grey shading represent residues that display at least 60% identity and at least

60% similarity, respectively. The underlined region represents the calponin homology (CH) region that spans approximately the first one hundred residues in the DUF1042 domain. **D) Electronic expression of SPATA4.** Using Genecards, SPATA4 is found to be widely expressed both experimentally (top panel, microarray) and electronically (lower two panels). However, note that although the experimental expression of SPATA4 by Genecards indicates that SPATA4 was not detected in testis, other studies have shown that SPATA4 is predominantly expressed in the testis.

Table 3.3: The percent identity of SPATA4 across 13 different species

	Bos taurus	Canis lupus familiaris	Ciona intestinalis	Danio rerio	Equus caballus	Gallus gallus	Homo sapiens	Macaca fascicularis	Macaca mulatta	Mus musculus	Oncorhynchus mykiss	Pan troglodytes	Rattus norvegicus
Bos taurus	-	-	-	-	-	-	-	-	-	-	-	-	-
Canis lupus familiaris	86	-	-	-	-	-	-	-	-	-	-	-	-
Ciona intestinalis	45	39	-	-	-	-	-	-	-	-	-	-	-
Danio rerio	51	50	63	-	-	-	-	-	-	-	-	-	-
Equus caballus	81	84	39	50	-	-	-	-	-	-	-	-	-
Gallus gallus	41	40	51	53	41	-	-	-	-	-	-	-	-
Homo sapiens	65	79	40	50	77	45	-	-	-	-	-	-	-
Macaca fascicularis	63	80	39	51	77	46	91	-		-	-	-	-
Macaca mulatta	63	80	41	50	76	46	91	99	-	-	-	-	-
Mus musculus	69	75	40	52	74	45	72	71	72	-	-	-	-
Oncorhynchus mykiss	52	49	55	78	52	52	45	44	44	51	-	-	-
Pan troglodytes	64	79	40	50	76	46	99	90	91	71	45	-	-
Rattus norvegicus	68	68	39	49	67	49	69	67	67	86	49	68	-

Table 3.3: The above table summarizes the percent identity of SPATA4 across 13 different species. Note that the species are listed in alphabetical order from left to right and from top to bottom.

3.4 *In vivo* coimmunoprecipitation of SPATA4 and sedlin

To begin characterizing the interaction between sedlin and SPATA4 a coimmunoprecipitation (CoIP) was performed. All experiments from this point onwards were performed with SPATA4 and sedlin from mouse. The CoIP was performed using lysates prepared from HEK 293T cells co-transfected with plasmids expressing myc-sedlin and FLAG-SPATA4. Sedlin and its binding partner were immunoprecipitated using rabbit anti-myc antibody, and the Western probed using mouse anti-myc antibody and mouse anti-FLAG antibody either simultaneously or separately. Both probing methods revealed that sedlin and SPATA4 do interact in mammalian cells under *in vivo* conditions (Figure 3.6A). Furthermore, it was seen that the expression of SPATA4 is stabilized by the co-expression of sedlin since a stronger band for SPATA4 was consistently observed when sedlin was present as compared to when SPATA4 was expressed alone. This latter observation further supports an interaction between sedlin and SPATA4.

Given that the interaction between sedlin and SPATA4 was detected using mammalian cells, and given that sedlin and C2L are components of the same protein complex, it was investigated whether SPATA4 interacts with C2L in mammalian cells. To this end another CoIP was performed as above except lysates were prepared from HEK 293T cells co-transfected with plasmids expressing myc-TRAPPC2L and FLAG-SPATA4. Western analysis was also done as above. In mammalian cells and under *in vivo* conditions, an interaction between C2L and SPATA4 was observed (Figure 3.6B). Furthermore, SPATA4 also appeared to be stabilized by the presence of C2L. Taken

together with the Y2H results, the CoIP experiments are consistent with an interaction between SPATA4 and TRAPP mediated by the sedlin protein.

In view of the fact that SPATA4 was shown to interact with both sedlin and C2L, we wanted to show that the latter interactions were specific and that SPATA4 is not a promiscuous binding protein. To this end another CoIP was performed as above using myc-ECT2 (421-883 aa) in place of either myc-sedlin or myc-TRAPPC2L, and the Western was also done as above. The epithelial cell transforming sequence 2 (ECT2) is a member of the Dbl family of guanine nucleotide exchange factor for Rho GTPases and is required for cytokinesis. An interaction was not observed between ECT2 (421-883 aa) and SPATA4 suggesting that the interaction between sedlin and SPATA4, and C2L and SPATA4 is specific (Figure 3.6C). Additionally, because the co-expression of myc-ECT2 (421-883 aa) with FLAG-SPATA4 was not seen to stabilize the expression of SPATA4 to the extent that either sedlin or C2L stabilized SPATA4, this further supports the notion that ECT2 does not interact with SPATA4.

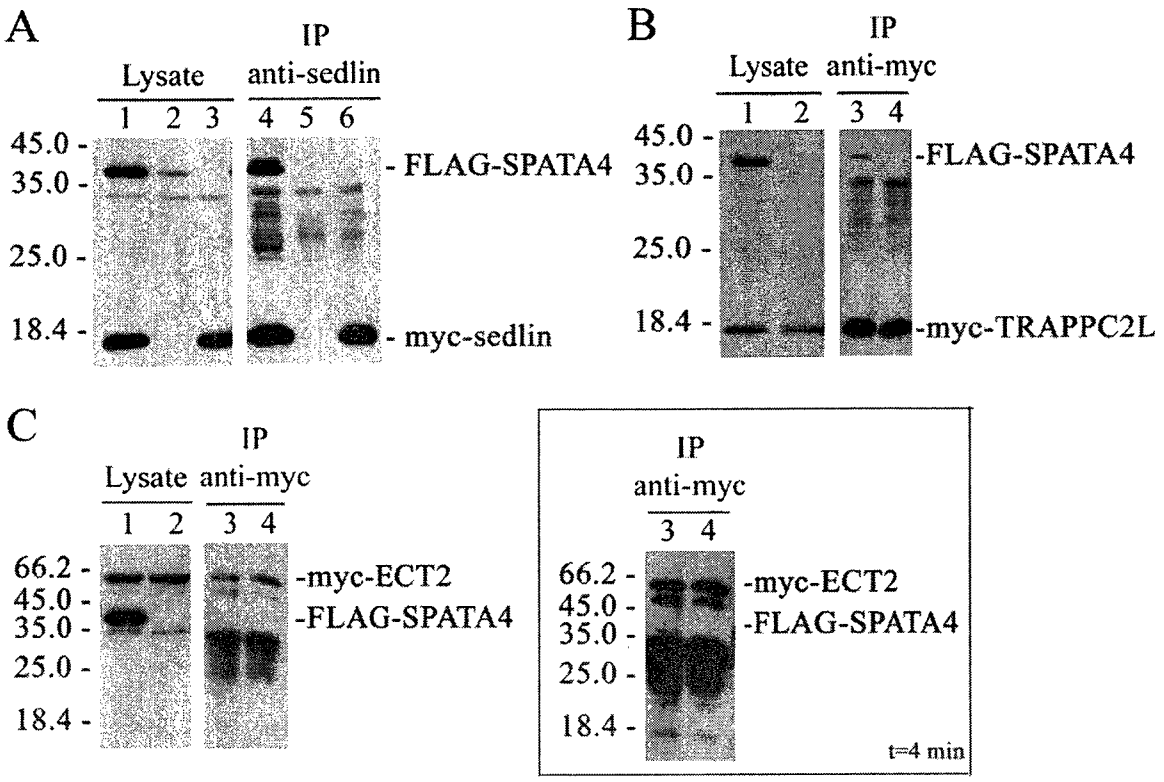

Figure 3.6: SPATA4 coimmunoprecipitates with both sedlin and C2L in HEK 293T cell lysates. Lysates were prepared from HEK 293T cells co-transfected with plasmids expressing: **A)** Lanes 1 and 4: FLAG-SPATA4 with myc-sedlin; Lanes 2 and 5: FLAG-SPATA4 with pRK5MYC; Lanes 3 and 6: pFLAGCMV6a with myc-sedlin; **B)** Lanes 1 and 3: FLAG-SPATA4 with myc-TRAPPC2L; Lanes 2 and 4: pFLAGCMV6a with myc-TRAPPC2L; **C)** Lanes 1 and 3: FLAG-SPATA4 with myc-ECT2 (421-883 aa); Lanes 2 and 4: pFLAGCMV6a with myc-ECT2 (421-883 aa). Samples were immunoprecipitated with 2 µg of rabbit anti-sedlin (panel A) or rabbit anti-myc (panels B and C) IgG on ice at 4°C for 16 hours, followed by incubation with 10 µl of Protein A-agarose on a nutator at 4°C for 2 hours. Samples were analyzed by Western blotting using mouse anti-myc and mouse anti-FLAG simultaneously both at a 1:5,000 dilution. Secondary antibody used was affinity purified peroxidase-labelled goat anti-mouse IgG at 1:10,000 dilution.

FLAG-SPATA4 is ~36 kDa, myc-sedlin is ~ 16 kDa and myc-ECT2 (421-883 aa) is ~ 53 kDa. Boxed panel shows lanes 3 and 4 CoIP samples at longer exposure time, t=4 minutes (compared to t=30 seconds for the corresponding CoIP samples). Even at t=4 minutes there is no sign of SPATA4 interacting with ECT2.

3.5 Gel Filtration of HEK 293T lysates reveals SPATA4 co-fractionates with assembled TRAPP complex

The CoIP results above suggested that SPATA4 binds to the TRAPP complex. When mammalian cell lysates are fractionated by size exclusion chromatography sedlin appears in two fractions: a high molecular weight fraction and a low molecular weight fraction. The former represents the TRAPP complex while the latter represents monomeric sedlin (Sacher and Ferro-Novick, 2001; Yamasaki et al., 2009). To examine which form of sedlin SPATA4 binds to, lysates from HEK 293T cells co-transfected with plasmids expressing myc-sedlin and FLAG-SPATA4 were fractionated by size exclusion chromatography. The resulting fractions were then analyzed by Western blotting using mouse anti-myc and mouse anti-FLAG. It was observed that sedlin is found in both the high and the low molecular weight fractions, consistent with previous findings. It was also found that SPATA4 co-fractionates with sedlin only in the high molecular weight fractions (Figure 3.7A) suggesting that SPATA4 physically interacts with TRAPP. The fact that SPATA4 was not observed to fractionate with sedlin in the low molecular weight fractions suggests that SPATA4 may not directly interact with sedlin, or that SPATA4 requires additional components to promote and stabilize the interaction between sedlin and SPATA4.

In addition, cell lysates of HEK 293T cells co-transfected with FLAGCMV6a and myc-sedlin or with FLAG-SPATA4 and pRK5MYC were prepared as above. When expressed on its own, myc-sedlin showed the expected results where sedlin was found to fractionate with both the high and the low molecular weight fractions (Figure 3.7B)

representing TRAPP and monomeric sedlin, respectively. Overexpression of only SPATA4 showed a weak band that co-fractionated with the TRAPP complex. This weak expression of SPATA4 in the absence of co-expressed sedlin is consistent with previous findings (refer to section 3.4) and further supports the notion that the presence of sedlin has a stabilizing effect on SPATA4 expression (Figure 3.7C). Taken together with the *in vivo* binding studies above, these results suggest that SPATA4 binds specifically to the TRAPP complex.

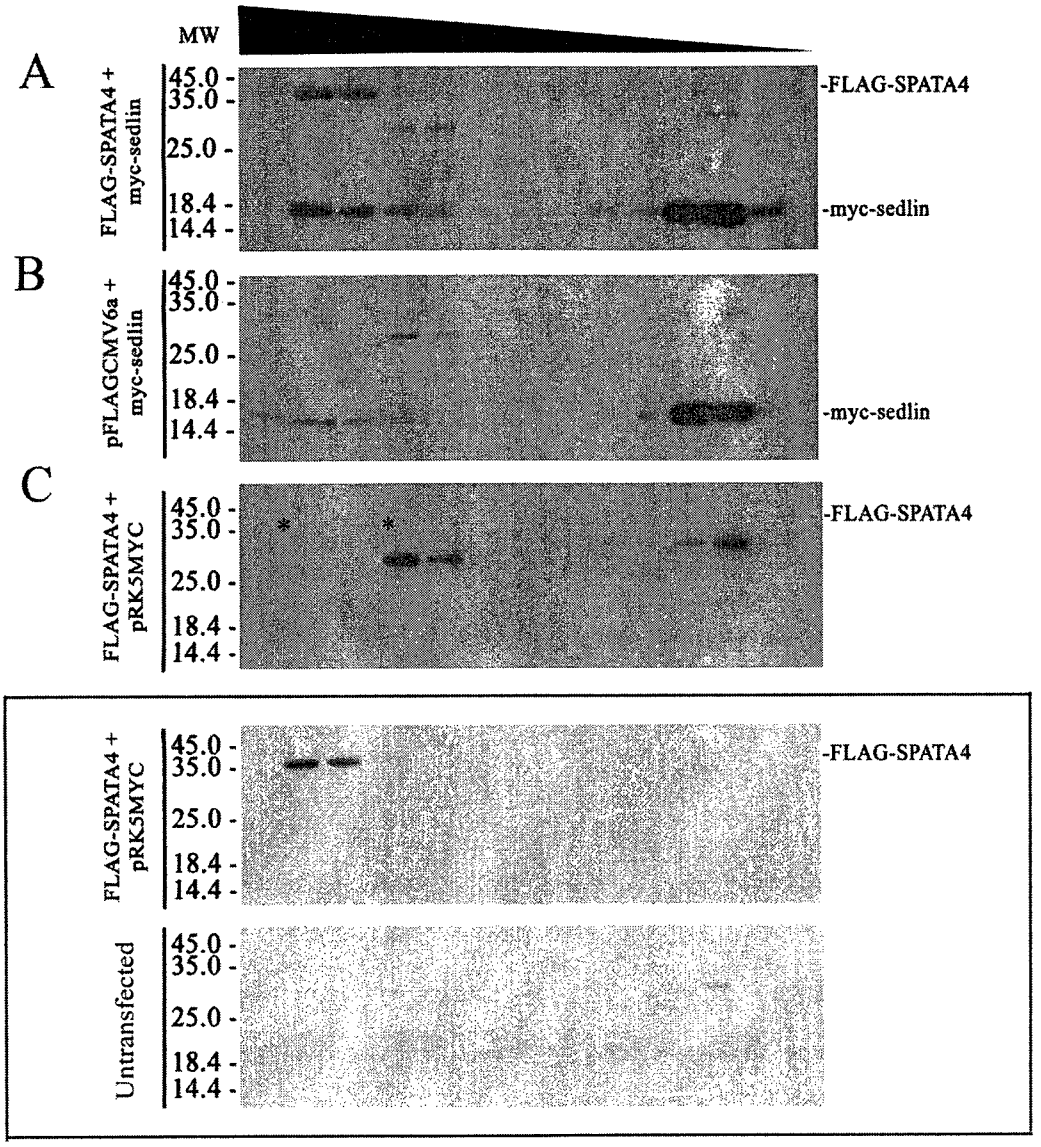

Figure 3.7: Gel Filtration showing SPATA4 physically interacts with TRAPP. Lysates were prepared from HEK 293T cells co-transfected with plasmids expressing: **A)** FLAG-SPATA4 with myc-sedlin; **B)** pFLAGCMV6a with myc-sedlin; **C)** FLAG-SPATA4 with pRK5MYC. Lysates were fractionated on a Superdex^{TM} 200 column and 0.5 ml fractions were collected. Fractions were analyzed by Western blotting using mouse anti-myc and mouse anti-FLAG simultaneously at a 1:5,000 dilution, followed by affinity purified antibody peroxidase-labelled goat anti-mouse IgG at a 1:10,000 dilution.

FLAG-SPATA4 is ~36 kDa and myc-sedlin is ~16 kDa. In Panel C the * marks the faint bands observed when FLAG-SPATA4 is not co-expressed with myc-sedlin. The top panel of the inset represents a repeat of the transfection performed in (C) to better show the SPATA4 bands, while the bottom panel shows the background bands that appear for untransfected HEK 293T cells. Note that the membranes in panels (A), (B) and (C) were exposed for 6 minutes while the membrane in the inset panels were exposed for 30 seconds.

3.6 *In vitro* binding assay suggests SPATA4 binds to sedlin in the TRAPP complex

It has previously been shown that sedlin in the monomeric form has minor structural differences compared to sedlin in the TRAPP complex (Kim et al., 2006; Jang et al., 2002b; Jang et al., 2002a) (Figure 3.8). To support the notion that SPATA4 binds to TRAPP and not monomeric sedlin as suggested by the gel filtration experiment above, an *in vitro* binding assay was performed using sedlin in its monomeric form as well as sedlin bound to its TRAPP partners TRAPPC3 and TRAPPC5. The proteins were purified from bacterial cell lysates expressing either MBP, MBP-SPATA4, His-sedlin or His-sedlin/TRAPPC3/TRAPPC5. Using His-sedlin, the binding assay samples contained 0.5 μM of either MBP or MBP-SPATA4 with increasing amounts (0, 0.1, 0.2, 0.5 μM) of His-sedlin. Consistent with the gel filtration result above, we could not detect an interaction between monomeric sedlin and SPATA4 as no increased binding of sedlin was detected when MBP-SPATA4 was used compared to MBP alone (Figure 3.9A). In contrast to monomeric sedlin, SPATA4 bound very efficiently to sedlin in the heterotrimeric complex of His-sedlin/TRAPPC3/TRAPPC5 (Figure 3.9B). The binding was so efficient that the concentrations of MBP, MBP-SPATA4 and the heterotrimeric complex were respectively reduced to 0.1 μM (former two proteins) and 0, 0.05, 0.1, 0.25 μM (latter proteins). These results support the notion that SPATA4 binds to TRAPP and not to monomeric sedlin. Therefore, the function of SPATA4 is likely carried out within the context of the TRAPP complex.

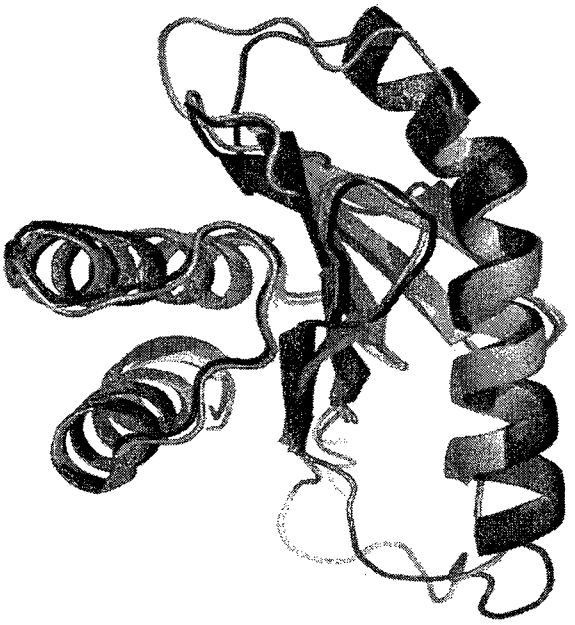

Figure 3.8: Overlay of sedlin in the heterotrimeric and monomeric state. When sedlin is in the heterotrimeric complex His-sedlin/TRAPPC3/TRAPPC5, sedlin contains 6.5 turns (dark blue) in the N-terminal α-helix compared to 4 turns when it is in the monomeric state (cyan). The above overlay shows that the additional turns are found at the beginning (bottom) and the end (top) of the N-terminal helix at residues 31-34 and 51-55, which correspond to the sequences KDDH and ENMWL, respectively.

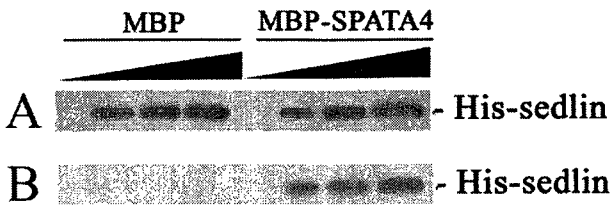

Figure 3.9: *In vitro* pulldown assays. MBP, MBP-SPATA4, a heterotrimeric His-sedlin/TRAPPC3/TRAPPC5 complex and His-sedlin were subjected to *in vitro* binding assay. *In vitro* assays contained either **A)** 0.5 μM of MBP or MBP-SPATA4 with increasing amounts of His-sedlin: 0, 0.1, 0.2, 0.5 μM or **B)** 0.1 μM of MBP or MBP-SPATA4 with increasing amounts of the heterotrimeric complex: 0, 0.05, 0.1, 0.25 μM. (Note that lower protein concentrations were used in B) in order to better observe the increased binding corresponding to increasing concentrations of sedlin.) Samples were allowed to bind for 1 hour at 4°C and pulldown employed 10 μl of amylose resin on a nutator for 1 hour at 4°C. Western analysis used affinity purified, polyclonal antibody recognizing sedlin at a dilution of 1:10,000 and affinity purified antibody peroxidase-labelled goat anti-rabbit IgG at 1:10,000 dilution. His-sedlin is ~ 16 kDa.

3.7 Mutations in sedlin do not affect the interaction with SPATA4

In light of the fact that over 30 different mutations in sedlin are known to cause the genetic skeletal disorder, SEDT (Savarirayan et al., 2003; Gecz et al., 2003), it was of interest to determine if mutations in sedlin affected the interaction with SPATA4. Perhaps mutations in sedlin affect sedlin's ability to properly interact with specific proteins, which would thus affect its ability to perform its function(s) within the cell. Subsequently, the inability of sedlin to perform its function(s) would trigger a cascade of events that would eventually result in SEDT. To this end, a yeast transformation was performed that introduced pGADT7-SPATA4 into an AH109 strain that contained pGBKT7-sedlin (D47Y), where the former plasmid is the prey plasmid containing SPATA4 that was rescued from the Y2H screen and the latter is the bait plasmid containing sedlin with a missense mutation at residue 47. The D47Y mutation in sedlin is significant because this mutation is one of the several documented missense mutations that is known to cause SEDT. After the transformation the cells were plated on DDO and TDO solid medium, where the TDO solid medium contained 1 mM of 3AT, and growth was observed on both plates. To better analyze the growth, three colonies were picked from the TDO solid medium and streaked on DDO solid medium to clean up the cells. One colony from each of the three streaks was subsequently grown and serial dilutions were spotted onto DDO and TDO solid medium. Growth on the DDO solid medium confirmed that all colonies contained both plasmids, while growth on the TDO solid medium indicated that the interaction between sedlin (D47Y) and SPATA4 was still present (Figure 3.10). Additionally, since the observed growth of AH109 cells containing

pGBKT7-sedlin (D47Y) with pGADT7-SPATA4 cells is comparable to the positive control (AH109 containing pGBKT7-sedlin and pGADT7-SPATA4), it does not appear that the interaction is either negatively or positively affected by the D47Y mutation in sedlin.

Since we were interested in determining if mutations in sedlin had an affect on its interaction with SPATA4, we did a second yeast transformation where pGADT7-SPATA4 was transformed into an AH109 strain containing pGBKT7-sedlin (APA). The latter sedlin mutation is not one of the mutations that lead to SEDT, however this mutation replaces the NPF motif of sedlin, where the NPF motif has been shown to mediate protein-protein interactions, more commonly by interaction with the epsin homology (EH) domain of various proteins (de Beer et al., 2000). The yeast transformation and spotting was performed as above and it was observed that the APA mutation of sedlin neither positively nor negatively affected the interaction with SPATA4 as compared with the positive control (Figure 3.10).

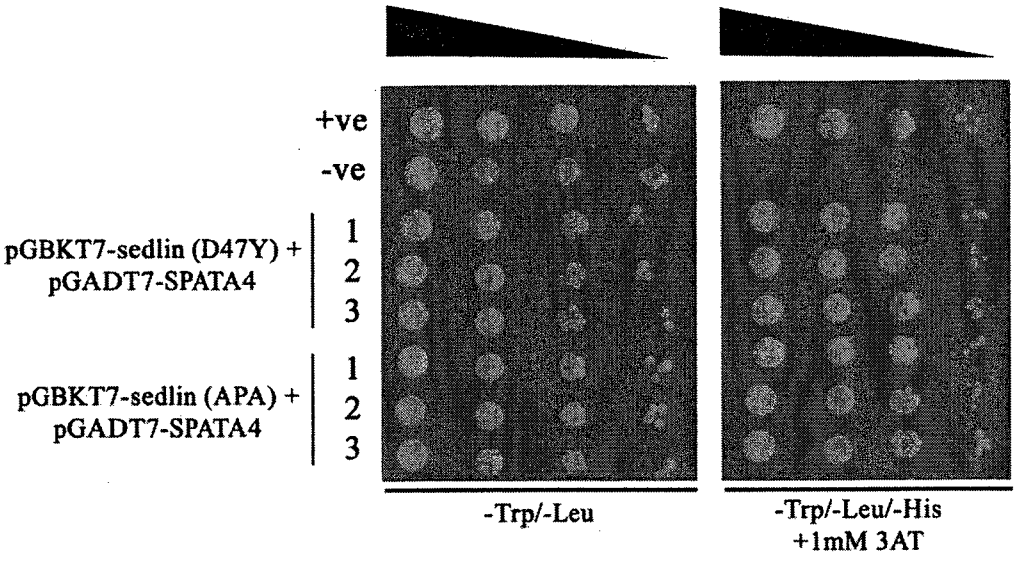

Figure 3.10: Mutations in sedlin do not affect the interaction with SPATA4. The yeast strain AH109 containing either pGBKT7-sedlin (D47Y) or pGBKT7-sedlin (APA) was transformed with the prey plasmid, pGADT7-SPATA4. Cells were grown on DDO and TDO solid medium and subsequent to colony growth, three colonies were chosen from the TDO solid medium and streaked on DDO solid medium. One colony from each of the three cleaned up streaks was then grown to an OD_{600} of 0.9 whereupon serial dilutions of 1/10, 1/100 and 1/1000 were made. The original and the diluted cultures were plated on DDO and TDO solid medium, where the left most column is the undiluted culture and the right most column is the most diluted. Looking at the TDO solid medium the interaction between both mutated forms of sedlin and SPATA4 appears unaffected as compared to the interaction observed in the positive control, which is the yeast strain AH109 containing pGBKT7-sedlin and pGADT7-SPATA4. The negative control is the yeast strain AH109 containing pGBKT7-TRAPPC2L with pGADT7-SPATA4.

4. Discussion

4.1 Sedlin and SPATA4 physically interact

This study describes a novel interaction between the TRAPP subunit sedlin and an uncharacterized protein called SPATA4. The gene encoding SPATA4 was discovered during a search for candidate apoptosis-related genes in mouse germ cells (Jiang et al., 2001). Thus far, very little is known about the SPATA4 protein. However, because SPATA4 is predominantly expressed in the testes (with the exception of rainbow trout and zebra fish in which SPATA4 is also found in the ovaries (Liu et al., 2005a; Liu et al., 2005b), it is thought to play a role in spermatogenesis and in the development of adult testes. Additionally, further support for this notion comes from gene expression studies that have found SPATA4 expression to be age dependent; SPATA4 is only expressed at sexual maturity and expression steadily increases with age whereupon when a certain age is reached the expression level remains constant (Liu et al., 2004a; Xie et al., 2007). Furthermore, SPATA4 appears to be an important protein in eukaryotes as it is conserved between human, rat, rainbow trout, zebra fish, chicken, chimpanzee, macaque, cow and ascidian (Liu et al., 2005c; Xie et al., 2007).

Using sedlin as the bait protein in a yeast two-hybrid screen, SPATA4 was obtained and selected for further characterization as SPATA4 showed specific interaction with sedlin but not with the sedlin-like protein TRAPPC2L (further detail concerning the

latter interaction is given in section 4.2). SPATA4 co-fractionates with the higher molecular weight TRAPP complex suggesting that it may bind to sedlin in the complex. Consistent with this notion, an *in vitro* pulldown assay revealed that the interaction of sedlin with SPATA4 may be enhanced and/or stabilized by the presence of sedlin's neighbouring TRAPP partners, TRAPPC3 and TRAPPC5. The observed increase in interaction may perhaps be explained by the fact that sedlin undergoes subtle conformational changes when in complex with TRAPPC3 and TRAPPC5 (Kim et al., 2006) compared to sedlin in the monomeric state (Jang et al., 2002a). In the monomeric state sedlin is composed of a mix of α-helices and one β-sheet, where the β-sheet (composed of five antiparallel β-strands) is sandwiched between an N-terminal α-helix on one side and two C-terminal anti-parallel α-helices on the other. In the heterotrimeric state, the overall structure of sedlin remains unchanged. However, the N-terminal α-helix of sedlin gains an additional 2.5 turns and thus contains 6.5 turns total. Perhaps it is the presence of the additional 2.5 turns that exposes amino acids and increases the specificity and binding of sedlin to SPATA4, and/or perhaps specific TRAPPC3 and/or TRAPPC5 residues also contribute to the binding. Crystallization of SPATA4 in complex with the heterotrimeric complex, His-sedlin/TRAPPC3/TRAPPC5 may provide insight into which residues and which TRAPP subunits participate in the interaction between sedlin and SPATA4. Moreover, crystallization may also reveal additional and/or confirm sedlin residues hypothesized to participate in protein-protein interactions and may further our understanding of sedlin's function in membrane trafficking and in the TRAPP complex.

From the above studies it is clear that sedlin and SPATA4 do indeed interact. However, the function that the two perform together is not yet apparent (hypothesized

functions are discussed below in sections 4.3 and 4.4). One way to study the function(s) of the two proteins is to perform localization studies using mammalian cells. By determining where the two proteins co-localize insight may be gained concerning where and how the two proteins function within a given cell. Studies have revealed that sedlin is found in the cytoplasm and at the Golgi (Sacher and Ferro-Novick, 2001; Yamasaki et al., 2009). Localization studies on overexpressed SPATA4 have found that SPATA4 localizes to the nucleus in COS-7 cells (Liu et al., 2004b). Although separately the two proteins appear to localize to different cellular compartments, small amounts of SPATA4 or sedlin may be in other cellular compartments. It would also be interesting to use sedlin-null mice and follow the expression pattern of SPATA4 with time as studies have shown that the expression of SPATA4 commences at the age of sexual maturity and increases with age (Liu et al., 2004a; Xie et al., 2007). Perhaps in sedlin-null mice, a decreased expression level of SPATA4 would be observed due to a lack of protein stability caused by the absence of sedlin. Alternatively, given that there is evidence of sedlin acting as a transcription factor (Ghosh et al., 2001) the reduced SPATA4 expression may be a result of reduced transcription levels of SPATA4.

4.2 TRAPPC2L interacts with SPATA4 via the TRAPP complex

TRAPPC2L is a novel sedlin-like protein that is hypothesized to compensate for the function of sedlin in SEDT patients (Scrivens et al., 2009). Therefore it was of interest to determine if C2L physically interacted with SPATA4. If C2L and SPATA4

interact then that would suggest the ability of C2L to compensate for sedlin in SEDT. However, if there is no interaction then that does not necessarily indicate the inability of C2L to compensate for sedlin. Rather, the latter occurrence may simply suggest that C2L is not able to fully compensate for sedlin, which may contribute to the explanation of why the SEDT phenotype is not as severe as expected given that sedlin is ubiquitously expressed (Scrivens et al., 2009). In this study the Y2H screen revealed that SPATA4 does not physically interact with C2L. However, the CoIP experiment revealed that C2L is able to immunoprecipitate SPATA4. These results suggest that C2L and SPATA4 interact via the TRAPP complex, where the physical interaction occurs between sedlin and SPATA4. The ability of C2L to immunoprecipitate, but not directly interact with, SPATA4 is consistent with a previous finding that showed that C2L and sedlin are part of the same TRAPP complex (Scrivens et al., 2009). In addition, the lack of physical interaction between SPATA4 and C2L provides support for a conserved functional divergence between C2L and sedlin. It will ultimately be of interest to determine what region of sedlin is responsible for the binding to SPATA4 and to determine if the same region is conserved within C2L. If the region is conserved, it would suggest that other factors such as TRAPPC3 and TRAPPC5 also participate in the interaction between sedlin and SPATA4 to promote and/or stabilize the binding since C2L is unable to physically bind SPATA4. A conserved region between the two proteins would also suggest residues important for any conserved function(s), folding, and/or binding that sedlin and C2L may share.

4.3 Implications in membrane trafficking

As previously mentioned, SPATA4 is an uncharacterized protein that has been suggested to have a function in spermatogenesis and gonad formation since several studies have found that it is predominantly expressed in the testis and that the expression level of SPATA4 appears to correlate with sexual maturity. To date, there has been no report for the involvement of SPATA4 in membrane trafficking. However, in light of the novel interaction between sedlin and SPATA4 and the data presented below, this study proposes that SPATA4 may be involved in membrane trafficking. A bioinformatic analysis of SPATA4 revealed that it contains a DUF1042 domain, and that within the human genome this domain is found in two other proteins. In SPATA4 the DUF1042 domain makes up ~50% of the protein. Of the two proteins that contain the DUF1042 domain one protein, SPEF1, was shown to bind to ZBED1. Interestingly, ZBED1 was found to bind to sedlin by Y2H. It is tempting to speculate that, if a ZBED1/SPEF1 complex binds to sedlin, the DUF1042 domain may in part mediate this interaction. Therefore, it would be of interest to test the involvement of the DUF1042 domain in binding to sedlin and in membrane traffic. In addition, TRAPP may have an as yet unidentified specialized role in spermatogenesis. Using mouse SPATA4- and SPEF1-null models, it would be of interest to observe the resulting phenotype and determine the effect on TRAPP localization and assembly. If TRAPP and/or TRAPP isocomplexes do play a specialized role in spermatogenesis then an observed defect in spermatogenesis in the above null models is hypothesized to correspond with an affected localization and/or assembly of TRAPP or TRAPP isocomplexes.

4.4 Implications in Disease

The goal of this study was to begin to characterize sedlin by identifying its interacting partners. In addition, the goal was also to use the obtained knowledge to gain insight into how mutations in sedlin lead to the genetic skeletal disorder, SEDT. Using a Y2H screen SPATA4 was discovered as a novel sedlin interactor and the interaction was verified using various biochemical methods. Initially, the interaction between sedlin and SPATA4 was not considered to have any relevance to SEDT since SEDT is a skeletal disorder, and thus far, there have been no reports of any testis-related issues in SEDT patients. However, further scrutiny of the interaction leads to some interesting links. It is known that SEDT manifests in early childhood at ~10-15 years of age, and it is also known that that age range coincides with the age where sexual maturity commences. Therefore, the manifestation of SEDT may be linked to the hormonal and/or chemical changes that occur in individuals upon the commencement of sexual maturity, where the latter has been linked to the expression levels of SPATA4. It is unknown how SPATA4 expression may influence the manifestation of SEDT. However given that both manifest at around the same age interval suggests there might be a link since sedlin interacts with SPATA4 and mutations in sedlin lead to SEDT. One documented missense mutation in sedlin is D47Y. It has been suggested that since the D47Y residue is exposed on the surface of sedlin that perhaps the mutation prevents sedlin from forming productive interactions which therefore leads to SEDT (Jang et al., 2002b). However, Y2H showed that the SPATA4-sedlin interaction was not affected by the D47Y mutation. It is possible that the Y2H system is not sensitive enough to pick up the difference in binding between

the sedlin D47Y mutant with SPATA4. To determine if there is a difference in binding strengths a more sensitive approach such as surface plasmon resonance (SPR) can be performed. Furthermore, if SPATA4 is linked to SEDT then perhaps there are one or more unobserved phenotypes in SEDT patients related to spermatogenesis or gonad development. One way to check this would be to test the expression level of SPATA4 in the testis and/or gonad of SEDT patients. As this is the first study to propose that SPATA4 is linked to SEDT, it is clear that further work remains to be done to characterize the relationship and dynamics between sedlin, SPATA4 and SEDT.

4.5. Future Perspectives

This study has shown a novel interaction between SPATA4 with a high molecular weight TRAPP complex. Furthermore, this interaction was found to be mediated through a physical interaction between sedlin and SPATA4 and suggests a link between SPATA4 and membrane traffic. A bioinformatic analysis of SPATA4 reveals the presence of a DUF1042 domain and also reveals another potential sedlin-interactor called SPEF1. SPEF1 is one of only three known human proteins to contain the DUF1042 domain, and may interact with sedlin via the formation of a heterodimeric complex containing SPEF1/ZBED1. If SPEF1 does indeed interact with sedlin then this interaction may provide the link that ties together vesicle tethering to Golgi-mediated traffic via the microtubules (Presley et al., 1997), since there is evidence that suggests an interaction between SPEF1 and microtubules via a CH domain (Dougherty et al., 2005).

Furthermore, both sedlin and SPEF1 are broadly expressed (Genecards) which may further support an interaction between the two proteins. As this is the first study to propose a link between vesicle tethering and Golgi-mediated trafficking via mictrotubules, further work remains to illuminate the mechanisms and intricacies of the relationship between the two transport pathways. It is certain that any insight gained will be transferable to similar cellular events and that such knowledge will increase the current understanding and knowledge of cross-talk and transport events within the cell.

Reference List

Aridor,M. and Hannan,L.A. (2000). Traffic jam: a compendium of human diseases that affect intracellular transport processes. Traffic. *1*, 836-851.

Aridor,M. and Hannan,L.A. (2002). Traffic jams II: an update of diseases of intracellular transport. Traffic. *3*, 781-790.

Barlowe,C. (1997). Coupled ER to Golgi transport reconstituted with purified cytosolic proteins. J. Cell Biol. *139*, 1097-1108.

Bielli,A., Haney,C.J., Gabreski,G., Watkins,S.C., Bannykh,S.I., and Aridor,M. (2005). Regulation of Sar1 NH2 terminus by GTP binding and hydrolysis promotes membrane deformation to control COPII vesicle fission. J. Cell Biol. *171*, 919-924.

Cai,H., Yu,S., Menon,S., Cai,Y., Lazarova,D., Fu,C., Reinisch,K., Hay,J.C., and Ferro-Novick,S. (2007). TRAPPI tethers COPII vesicles by binding the coat subunit Sec23. Nature *445*, 941-944.

Cai,H., Zhang,Y., Pypaert,M., Walker,L., and Ferro-Novick,S. (2005). Mutants in trs120 disrupt traffic from the early endosome to the late Golgi. J. Cell Biol. *171*, 823-833.

Cai,Y., Chin,H.F., Lazarova,D., Menon,S., Fu,C., Cai,H., Sclafani,A., Rodgers,D.W., De La Cruz,E.M., Ferro-Novick,S., and Reinisch,K.M. (2008). The structural basis for activation of the Rab Ypt1p by the TRAPP membrane-tethering complexes. Cell *133*, 1202-1213.

Cavanaugh,L.F., Chen,X., Richardson,B.C., Ungar,D., Pelczer,I., Rizo,J., and Hughson,F.M. (2007). Structural analysis of conserved oligomeric Golgi complex subunit 2. J. Biol. Chem. *282*, 23418-23426.

Chan S.W., Fowler,K.J., Choo,A., and Kalitsis,P. (2005). Spef1, a conserved novel testis protein found in sperm flagella. Gene *353*, 189-199.

Chiari,R., Foury,F., De,P.E., Baurain,J.F., Thonnard,J., and Coulie,P.G. (1999). Two antigens recognized by autologous cytolytic T lymphocytes on a melanoma result from a single point mutation in an essential housekeeping gene. Cancer Res. *59*, 5785-5792.

de Beer,T., Hoofnagle,A.N., Enmon,J.L., Bowers,R.C., Yamabhai,M., Kay,B.K., and Overduin,M. (2000). Molecular mechanism of NPF recognition by EH domains. Nat. Struct. Biol. *7*, 1018-1022.

Dong,G., Hutagalung,A.H., Fu,C., Novick,P., and Reinisch,K.M. (2005). The structures of exocyst subunit Exo70p and the Exo84p C-terminal domains reveal a common motif. Nat. Struct. Mol. Biol. *12*, 1094-1100.

Dougherty,G.W., Adler,H.J., Rzadzinska,A., Gimona,M., Tomita,Y., Lattig,M.C., Merritt,R.C., Jr., and Kachar,B. (2005). CLAMP, a novel microtubule-associated protein with EB-type calponin homology. Cell Motil. Cytoskeleton *62*, 141-156.

Dumas,J.J., Merithew,E., Sudharshan,E., Rajamani,D., Hayes,S., Lawe,D., Corvera,S., and Lambright,D.G. (2001). Multivalent endosome targeting by homodimeric EEA1. Mol. Cell *8*, 947-958.

Fan,L., Yu,W., and Zhu,X. (2003). Interaction of Sedlin with chloride intracellular channel proteins. FEBS Lett. *540*, 77-80.

Fasshauer,D., Sutton,R.B., Brunger,A.T., and Jahn,R. (1998). Conserved structural features of the synaptic fusion complex: SNARE proteins reclassified as Q- and R-SNAREs. Proc. Natl. Acad. Sci. U. S. A *95*, 15781-15786.

Fields,S. and Song,O. (1989). A novel genetic system to detect protein-protein interactions. Nature *340*, 245-246.

Gecz,J., Hillman,M.A., Gedeon,A.K., Cox,T.C., Baker,E., and Mulley,J.C. (2000). Gene structure and expression study of the SEDL gene for spondyloepiphyseal dysplasia tarda. Genomics *69*, 242-251.

Gecz,J., Shaw,M.A., Bellon,J.R., and de Barros,L.M. (2003). Human wild-type SEDL protein functionally complements yeast Trs20p but some naturally occurring SEDL mutants do not. Gene *320*, 137-144.

Gedeon,A.K., Colley,A., Jamieson,R., Thompson,E.M., Rogers,J., Sillence,D., Tiller,G.E., Mulley,J.C., and Gecz,J. (1999). Identification of the gene (SEDL) causing X-linked spondyloepiphyseal dysplasia tarda. Nat. Genet. *22*, 400-404.

Gedeon,A.K., Tiller,G.E., Le,M.M., Heuertz,S., Tranebjaerg,L., Chitayat,D., Robertson,S., Glass,I.A., Savarirayan,R., Cole,W.G., Rimoin,D.L., Kousseff,B.G., Ohashi,H., Zabel,B., Munnich,A., Gecz,J., and Mulley,J.C. (2001). The molecular basis of X-linked spondyloepiphyseal dysplasia tarda. Am. J. Hum. Genet. *68*, 1386-1397.

Ghosh,A.K., Majumder,M., Steele,R., White,R.A., and Ray,R.B. (2001). A novel 16-kilodalton cellular protein physically interacts with and antagonizes the functional activity of c-myc promoter-binding protein 1. Mol. Cell Biol. *21*, 655-662.

Ghosh,A.K., Steele,R., and Ray,R.B. (2003). Modulation of human luteinizing hormone beta gene transcription by MIP-2A. J. Biol. Chem. *278*, 24033-24038.

Gissen,P., Johnson,C.A., Morgan,N.V., Stapelbroek,J.M., Forshew,T., Cooper,W.N., McKiernan,P.J., Klomp,L.W., Morris,A.A., Wraith,J.E., McClean,P., Lynch,S.A., Thompson,R.J., Lo,B., Quarrell,O.W., Di,R.M., Trembath,R.C., Mandel,H., Wali,S., Karet,F.E., Knisely,A.S., Houwen,R.H., Kelly,D.A., and Maher,E.R. (2004). Mutations

in VPS33B, encoding a regulator of SNARE-dependent membrane fusion, cause arthrogryposis-renal dysfunction-cholestasis (ARC) syndrome. Nat. Genet. *36*, 400-404.

Gonzalez,L.C., Jr., Weis,W.I., and Scheller,R.H. (2001). A novel snare N-terminal domain revealed by the crystal structure of Sec22b. J. Biol. Chem. *276*, 24203-24211.

Harper,P.S. (1996). New genes for old diseases: the molecular basis of myotonic dystrophy and Huntington's disease. The Lumleian Lecture 1995. J. R. Coll. Physicians Lond *30*, 221-231.

Hubsman,M., Yudkovsky,G., and Aronheim,A. (2001). A novel approach for the identification of protein-protein interaction with integral membrane proteins. Nucleic Acids Res. *29*, E18.

Jang,S.B., Cho,Y.S., Eom,S.J., Choi,E.J., Kim,K.H., Suh,P.G., and Oh,B.H. (2002a). Crystallization and preliminary X-ray crystallographic analysis of SEDL. Acta Crystallogr. D. Biol. Crystallogr. *58*, 564-566.

Jang,S.B., Kim,Y.G., Cho,Y.S., Suh,P.G., Kim,K.H., and Oh,B.H. (2002b). Crystal structure of SEDL and its implications for a genetic disease spondyloepiphyseal dysplasia tarda. J. Biol. Chem. *277*, 49863-49869.

Jiang,H., Li,L.Y., and Lu,G.X. (2001). Molecular Cloning of Genes Related to Apoptosis in Spermatogenic Cells of Mouse. Sheng Wu Hua Xue. Yu Sheng Wu Wu Li Xue. Bao. (Shanghai) *33*, 421-425.

Jiang,Y., Scarpa,A., Zhang,L., Stone,S., Feliciano,E., and Ferro-Novick,S. (1998). A high copy suppressor screen reveals genetic interactions between BET3 and a new gene. Evidence for a novel complex in ER-to-Golgi transport. Genetics *149*, 833-841.

Jones,S., Newman,C., Liu,F., and Segev,N. (2000). The TRAPP complex is a nucleotide exchanger for Ypt1 and Ypt31/32. Mol. Biol. Cell *11*, 4403-4411.

Kim,Y.G., Raunser,S., Munger,C., Wagner,J., Song,Y.L., Cygler,M., Walz,T., Oh,B.H., and Sacher,M. (2006). The architecture of the multisubunit TRAPP I complex suggests a model for vesicle tethering. Cell *127*, 817-830.

Liu,B., Liu,S., He,S., Zhao,Y., Hu,H., and Wang,Z. (2005a). Cloning and expression analysis of gonadogenesis-associated gene SPATA4 from rainbow trout (Oncorhynchus mykiss). J. Biochem. Mol. Biol. *38*, 206-210.

Liu,S., Liu,B., He,S., Zhao,Y., and Wang,Z. (2005b). Cloning and characterization of zebra fish SPATA4 gene and analysis of its gonad specific expression. Biochemistry (Mosc.) *70*, 638-644.

Liu,S.F., Ai,C., Ge,Z.Q., Liu,H.L., Liu,B.W., He,S., and Wang,Z. (2005c). Molecular cloning and bioinformatic analysis of SPATA4 gene. J. Biochem. Mol. Biol. *38*, 739-747.
Liu,S.F., He,S., Liu,B.W., Zhao,Y., and Wang,Z. (2004a). Cloning and characterization of testis-specific spermatogenesis associated gene homologous to human SPATA4 in rat. Biol. Pharm. Bull. *27*, 1867-1870.

Liu,S.F., Lu,G.X., Liu,G., Xing,X.W., Li,L.Y., and Wang,Z. (2004b). Cloning of a full-length cDNA of human testis-specific spermatogenic cell apoptosis inhibitor TSARG2 as a candidate oncogene. Biochem. Biophys. Res. Commun. *319*, 32-40.

Lowe,M. (2000). Membrane transport: tethers and TRAPPs. Curr. Biol. *10*, R407-R409.

Macdonald,M.E., Ambrose,C.M., Duyao,M.P., Myers,R.H., Lin,C., Srinidhi,L., Barnes,G., Taylor,S.A., James,M., Groot,N., Macfarlane,H., Jenkins,B., Anderson,M.A., Wexler,N.S., Gusella,J.F., Bates,G.P., Baxendale,S., Hummerich,H., Kirby,S., North,M., Youngman,S., Mott,R., Zehetner,G., Sedlacek,Z., Poustka,A., Frischauf,A.M., Lehrach,H., Buckler,A.J., Church,D., Doucettestamm,L., Odonovan,M.C., Ribaramirez,L., Shah,M., Stanton,V.P., Strobel,S.A., Draths,K.M., Wales,J.L., Dervan,P., Housman,D.E., Altherr,M., Shiang,R., Thompson,L., Fielder,T., Wasmuth,J.J., Tagle,D., Valdes,J., Elmer,L., Allard,M., Castilla,L., Swaroop,M., Blanchard,K., Collins,F.S., Snell,R., Holloway,T., Gillespie,K., Datson,N., Shaw,D., and Harper,P.S. (1993). A Novel Gene Containing A Trinucleotide Repeat That Is Expanded and Unstable on Huntingtons-Disease Chromosomes. Cell *72*, 971-983.

MacKenzie,J.J., Fitzpatrick,J., Babyn,P., Ferrero,G.B., Ballabio,A., Billingsley,G., Bulman,D.E., Strasberg,P., Ray,P.N., and Costa,T. (1996). X linked spondyloepiphyseal dysplasia: a clinical, radiological, and molecular study of a large kindred. J. Med. Genet. *33*, 823-828.

Markgraf,D.F., Peplowska,K., and Ungermann,C. (2007). Rab cascades and tethering factors in the endomembrane system. FEBS Lett. *581*, 2125-2130.

Matsuoka,K., Orci,L., Amherdt,M., Bednarek,S.Y., Hamamoto,S., Schekman,R., and Yeung,T. (1998). COPII-coated vesicle formation reconstituted with purified coat proteins and chemically defined liposomes. Cell *93*, 263-275.

Morozova,N., Liang,Y., Tokarev,A.A., Chen,S.H., Cox,R., Andrejic,J., Lipatova,Z., Sciorra,V.A., Emr,S.D., and Segev,N. (2006). TRAPPII subunits are required for the specificity switch of a Ypt-Rab GEF. Nat. Cell Biol. *8*, 1263-1269.

Moyer,B.D., Allan,B.B., and Balch,W.E. (2001). Rab1 interaction with a GM130 effector complex regulates COPII vesicle cis--Golgi tethering. Traffic. *2*, 268-276.
Munro,S. and Pelham,H.R. (1987). A C-terminal signal prevents secretion of luminal ER proteins. Cell *48*, 899-907.

Nielsen,E., Christoforidis,S., Uttenweiler-Joseph,S., Miaczynska,M., Dewitte,F., Wilm,M., Hoflack,B., and Zerial,M. (2000). Rabenosyn-5, a novel Rab5 effector, is complexed with hVPS45 and recruited to endosomes through a FYVE finger domain. J. Cell Biol. *151*, 601-612.

Nilsson,T., Jackson,M., and Peterson,P.A. (1989). Short cytoplasmic sequences serve as retention signals for transmembrane proteins in the endoplasmic reticulum. Cell *58*, 707-718.

Pfeffer,S.R. (1996). Transport vesicle docking: SNAREs and associates. Annu. Rev. Cell Dev. Biol. *12*, 441-461.

Pfeffer,S.R. (1999). Transport-vesicle targeting: tethers before SNAREs. Nat. Cell Biol. *1*, E17-E22.

Presley,J.F., Cole,N.B., Schroer,T.A., Hirschberg,K., Zaal,K.J., and Lippincott-Schwartz,J. (1997). ER-to-Golgi transport visualized in living cells. Nature *389*, 81-85.

Rossi,G., Kolstad,K., Stone,S., Palluault,F., and Ferro-Novick,S. (1995). BET3 encodes a novel hydrophilic protein that acts in conjunction with yeast SNAREs. Mol. Biol. Cell *6*, 1769-1780.

Sacher,M. (2003). Membrane traffic fuses with cartilage development. FEBS Lett. *550*, 1-4.

Sacher,M., Barrowman,J., Schieltz,D., Yates,J.R., III, and Ferro-Novick,S. (2000). Identification and characterization of five new subunits of TRAPP. Eur. J. Cell Biol. *79*, 71-80.

Sacher,M., Barrowman,J., Wang,W., Horecka,J., Zhang,Y., Pypaert,M., and Ferro-Novick,S. (2001). TRAPP I implicated in the specificity of tethering in ER-to-Golgi transport. Mol. Cell *7*, 433-442.

Sacher,M. and Ferro-Novick,S. (2001). Purification of TRAPP from Saccharomyces cerevisiae and identification of its mammalian counterpart. Methods Enzymol. *329*, 234-241.

Sacher,M., Jiang,Y., Barrowman,J., Scarpa,A., Burston,J., Zhang,L., Schieltz,D., Yates,J.R., III, Abeliovich,H., and Ferro-Novick,S. (1998). TRAPP, a highly conserved novel complex on the cis-Golgi that mediates vesicle docking and fusion. EMBO J. *17*, 2494-2503.

Sacher,M., Kim,Y.G., Lavie,A., Oh,B.H., and Segev,N. (2008). The TRAPP complex: insights into its architecture and function. Traffic. *9*, 2032-2042.

Savarirayan,R., Thompson,E., and Gecz,J. (2003). Spondyloepiphyseal dysplasia tarda (SEDL, MIM #313400). Eur. J. Hum. Genet. *11*, 639-642.

Scrivens,P.J., Shahrzad,N., Moores,A., Morin,A., Brunet,S., and Sacher,M. (2009). TRAPPC2L is a novel, highly conserved TRAPP-interacting protein. Traffic. *10*, 724-736.

Sironen,A., Thomsen,B., Andersson,M., Ahola,V., and Vilkki,J. (2006). An intronic insertion in KPL2 results in aberrant splicing and causes the immotile short-tail sperm defect in the pig. Proc. Natl. Acad. Sci. U. S. A *103*, 5006-5011.

Sivaram,M.V., Furgason,M.L., Brewer,D.N., and Munson,M. (2006). The structure of the exocyst subunit Sec6p defines a conserved architecture with diverse roles. Nat. Struct. Mol. Biol. *13*, 555-556.

Smith,R., Klein,P., Koc-Schmitz,Y., Waldvogel,H.J., Faull,R.L., Brundin,P., Plomann,M., and Li,J.Y. (2007). Loss of SNAP-25 and rabphilin 3a in sensory-motor cortex in Huntington's disease. J. Neurochem. *103*, 115-123.

Sonnichsen,B., Lowe,M., Levine,T., Jamsa,E., Dirac-Svejstrup,B., and Warren,G. (1998). A role for giantin in docking COPI vesicles to Golgi membranes. J. Cell Biol. *140*, 1013-1021.

Stagljar,I., Korostensky,C., Johnsson,N., and te,H.S. (1998). A genetic system based on split-ubiquitin for the analysis of interactions between membrane proteins in vivo. Proc. Natl. Acad. Sci. U. S. A *95*, 5187-5192.

Taybi,H. and Lachman,R.S. (1996). Radiology of syndromes, metabolic disorders, and skeletal dysplasias. (St. Louis: Mosby-Year Book Inc.).

Tochio,H., Tsui,M.M., Banfield,D.K., and Zhang,M. (2001). An autoinhibitory mechanism for nonsyntaxin SNARE proteins revealed by the structure of Ykt6p. Science *293*, 698-702.

Tremblay,J.J. and Drouin,J. (1999). Egr-1 is a downstream effector of GnRH and synergizes by direct interaction with Ptx1 and SF-1 to enhance luteinizing hormone beta gene transcription. Mol. Cell Biol. *19*, 2567-2576.

Wang,W. and Ferro-Novick,S. (2002). A Ypt32p exchange factor is a putative effector of Ypt1p. Mol. Biol. Cell *13*, 3336-3343.

Wang,W., Sacher,M., and Ferro-Novick,S. (2000). TRAPP stimulates guanine nucleotide exchange on Ypt1p. J. Cell Biol. *151*, 289-296.

Waters,M.G. and Hughson,F.M. (2000). Membrane tethering and fusion in the secretory and endocytic pathways. Traffic. *1*, 588-597.

Whyte,J.R. and Munro,S. (2002). Vesicle tethering complexes in membrane traffic. J. Cell Sci. *115*, 2627-2637.

Xie,M.C., Ai,C., Jin,X.M., Liu,S.F., Tao,S.X., Li,Z.D., and Wang,Z. (2007). Cloning and characterization of chicken SPATA4 gene and analysis of its specific expression. Mol. Cell Biochem. *306*, 79-85.

Yamasaki,A., Menon,S., Yu,S., Barrowman,J., Meerloo,T., Oorschot,V., Klumperman,J., Satoh,A., and Ferro-Novick,S. (2009). mTrs130 is a component of a mammalian TRAPPII complex, a Rab1 GEF that binds to COPI-coated vesicles. Mol. Biol. Cell *20*, 4205-4215.

Yu,S., Satoh,A., Pypaert,M., Mullen,K., Hay,J.C., and Ferro-Novick,S. (2006). mBet3p is required for homotypic COPII vesicle tethering in mammalian cells. J. Cell Biol. *174*, 359-368.

Yuce,O., Piekny,A., and Glotzer,M. (2005). An ECT2-centralspindlin complex regulates the localization and function of RhoA. J. Cell Biol. *170*, 571-582.